The Pennsylvania State University

The Graduate School

Department of Mechanical and Nuclear Engineering

CHARACTERIZATION OF PRE- AND POST-BREAKUP LIQUID JETS

A Thesis in

Nuclear Engineering

by

Daniel Jacob Skilone

Submitted in Partial Fulfillment
of the Requirements
for the Degree of

Master of Science

May 2009

The thesis of Daniel Jacob Skilone was reviewed and approved* by the following:

Seungjin Kim
Assistant Professor of Mechanical and Nuclear Engineering
Thesis Advisor

Kostadin Ivanov
Distinguished Professor of Nuclear Engineering

Jack Brenizer
J. “Lee” Everett Professor of Mechanical and Nuclear Engineering
Chair of Nuclear Engineering

*Signatures are on file in the Graduate School

ABSTRACT

The formation and disintegration of liquid jets has been studied for over 150 years due to its importance in many engineering applications including the nuclear reactor. As most applications involve the transfer of mass, momentum, and energy under adverse conditions, an understanding of the mechanisms governing the formation and disintegration of jets, as well as the different geometries encountered by jets is of paramount importance for ensuring safety, efficiency, and predictability.

Literature describes a number of models and correlations regarding very specific areas within the overall subject of jet disintegration. However, there are very few instances where this information is combined to provide a more holistic view of this phenomenon. The present work integrates available correlations and experimental data and develops predictive methods important for mass, momentum, and energy transfer.

Based upon the observations and recommendations of previous work, the present work encompasses turbulent liquid jets in the Rayleigh and first wind-induced breakup regimes. Detailed analyses and the resulting expressions of the surface area for the continuous jet and disintegrated drop regions in these regimes are provided. Hence, the present analysis proposes a mechanistic methodology to characterize the pre- and post-breakup geometries of a liquid jet in engineering applications.

TABLE OF CONTENTS

LIST OF FIGURES

LIST OF TABLES

NOMENCLATURE

Acronyms

FWI:	First Wind-Induced
SWI:	Second Wind-Induced

Symbols

$\dot{q}_l'''$	Heat generation rate in the liquid
A	Surface area of the jet
a	Undisturbed jet radius
b_n	Constant in a fourier series
c_p	Specific heat of the jet liquid
C	Constant in a Stanton number correlation
c_1	Empirical constant relating jet diameter and disturbance size
c_2	Empirical value for average number of drops per unit length
D	Diameter of a drop formed upon jet breakup
d_d	Diameter of drops present after breakup
d_{jet}	Diameter of jet
D_n	Number geometric mean drop size
d_o	Undisturbed jet diameter

d_{smd}	Sauter mean diameter of drops
f	Functional representation of a disturbance
f_o	Amplitude function describing a disturbance
g	Gravitational constant
i_l	Liquid enthalpy of the jet
k	Constant applied to the undisturbed diameter
L	Total axial length of jet under consideration
l_1	Rayleigh or FWI continuous region length
l_2	Rayleigh discontinuous region or FWI surface disturbance region length
l_3	FWI discontinuous region length
l_b	Axial length of jet required for breakup following issue
l_{jet}	Axial length of jet.
N	Number of drops of a given diameter
n_d	Number of drops present after breakup
n_i	Any positive real integrer, including zero
n_w	Number of waves in the surface disturbance region
p	Perimeter of an ellipse
P	Potential surface energy
q	Exponential growth rate of a disturbance
q_{max}	Exponential growth rate of the most dangerous disturbance
r	Disturbed jet radius
Re_{crit}	Critical Reynolds number for laminar/turbulent transition
s_g	Standard deviation of actual drop size from the mean value

t	Age of the jet from a the issuing nozzle
t_b	Time required for jet breakup following issue
T_g	Temperature of the gaseous environment
T_o	Temperature of the at the nozzle exit
T_x	Temperature of the jet at distance x
u	Velocity of the jet
$\bar{u}_l$	Velocity vector of the jet
x	Streamwise distance from the issuing nozzle
y	Cross-stream length of a disturbance
z	Streamwise length of a disturbance

Greek Symbols

Γ	Mass transfer rate between jet and environment
γ	Dimensionless wave number of a disturbance
Λ	Cross-stream autocorrelation distance
λ	Wavelength of the disturbance
λ_{max}	Wavelength of the most dangerous disturbance
ε	Drop or disturbance ellipsicity
$\bar{\varepsilon}$	Average drop or disturbance ellipsicity
ε_H	Eddy diffusivity of heat
ν	Liquid kinematic viscosity of the jet

μ	Liquid viscosity of the jet
μ_g	Vapor viscosity of the jet environment
ρ	Liquid density of the jet
ρ_g	Vapor density of the jet environment
σ	Surface tension of the jet

Dimensionless Groups

Oh	Ohnesorge Number	$Oh = \frac{\mu}{(\rho \sigma d)^{0.5}}$
Re/*Re*$_l$	Liquid Reynolds Number	$Re = \frac{\rho u d}{\mu}$
Re$_{smd}$	Sauter Mean Drop Reynolds Number	$Re = \frac{\rho u_d d_{smd}}{\mu}$
St	Stanton Number	$St = \frac{i_l}{\rho c_p u}$
We/*We*$_l$	Liquid Weber Number	$We = \frac{\rho u^2 d}{\sigma}$
We$_g$/*We*$_A$	Vapor Weber Number	$We_g = \frac{\rho_g u^2 d}{\sigma}$
We$_{smd}$	Sauter Mean Drop Weber Number	$We_g = \frac{\rho_g u_d{}^2 d_{smd}}{\sigma}$

ACKNOWLEDGEMENTS

I would like to thank my advisors, Professors Lawrence Hochreiter and Seungjin Kim, for the time, support, and guidance they provided me as a graduate student. Their backgrounds and experience in both thermal hydraulics and life in general have provided me with a number of informative lessons, important information, and fond memories. I would also like to thank Professor Kostadin Ivanov and Program Chair Jack Brenizer for their time with this work.

I also wish to acknowledge the support of my family and friends. My parents, Becky and Ed Elnikar, my fiancée, Rachel Snatchko, and my long-time friend, Mike Meholic, have all provided me with an invaluable amount of support, understanding, and encouragement throughout my graduate (and undergraduate) studies. I would also like to thank my officemates, both present and past, for their camaraderie, companionship, and conversations.

Chapter 1

Introduction

Liquid jets are encountered in a wide variety of disciplines. Diesel engines [46], mixing-type heat exchangers [44], thermal degasifiers [1], and sea-water desalinators [18] all involve the use of a pressure-driven injection device that produces a liquid jet at the nozzle exit. In the realm of nuclear engineering, light water reactors can encounter liquid jets when cooling water enters larger piping from smaller, connecting piping during postulated severe accidents [59], molten core jets can also appear in light water reactors under similar severe conditions, and high-pressure water is released as a liquid jet into sodium when steam generator tubes fail in sodium-cooled reactors [45].

The aforementioned are certainly not an all-inclusive list of liquid jet applications; rather they represent a multitude of applications in which a liquid jet acts as a vehicle for mass, momentum, and energy to be exchanged in some manner. Understanding the exchange of thermal energy in particular is paramount to ensuring safety and efficiency, regardless of the application. In most analyses, thermal energy exchange or heat transfer is customarily characterized by the in- and out-flows of thermal energy, which are surface phenomena [19]. In this manner, heat transfer is associated exclusively with processes occurring at a well-defined control surface and is therefore proportional to a surface area. Thus, it is logical to

suggest that an understanding of the thermal energy exchange between a liquid jet and the environment surrounding it is predicated upon the ability to characterize the interface over which transport occurs – namely the surface area of the jet.

The images in Figure 1-1 provide an example of four distinctly different states that could be encountered by a liquid jet [21]. The range of conditions inherent to the production of these images is rather large and is representative of the practical range of liquid jet production. The stark disparity between the depicted states implies that the heat transfer interface linking a liquid jet and its environment is dynamic in nature. With that in mind, the primary challenge to quantifying the heat transfer becomes the accurate description of the jet surface area for a given set of conditions.

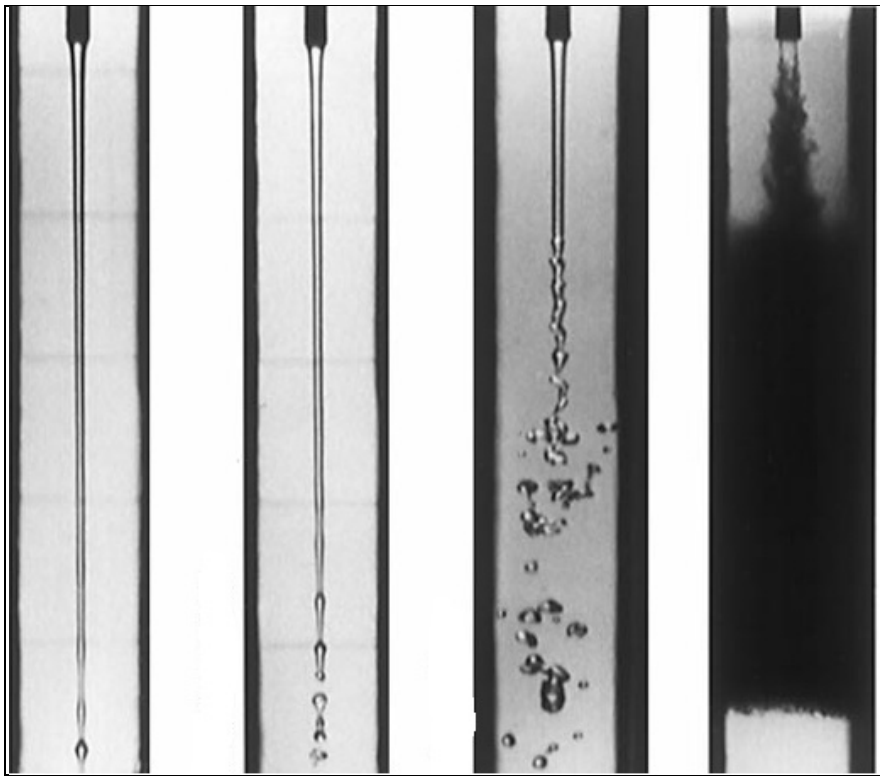

Figure 1-1: Multiple modes of liquid jet disintegration [21].

It is immediately apparent that, given the conditions depicted in Figure 1-1, a liquid jet will break up or disintegrate at some distance away from the issuing nozzle. The variable nature of this distance suggests a need to predict the continuous or un-broken length of a liquid jet under a range of conditions. It is also evident from Figure 1-1 that the geometries pre- and post-break up are radically different. What begins as a straight, coherent jet is observed to become disturbed at some point. However, this disturbance appears to manifest itself in a number of different modes.

In the first image, the continuous jet becomes disturbed at some distance and undergoes a change causing a capillary or thinning deformation. This deformation results in the formation of a single drop that is proportional to the undisturbed jet diameter.

The second image illustrates the production of varicose or swollen disturbances following the capillary deformation of the jet. This deformation also results in the formation of a single drop; however, it appears to occur at a comparatively decreased distance from the nozzle exit and the size of the drop produced is varied.

The third image no longer exhibits any large-scale capillary deformation of the jet. Rather, the varicose disturbances are far more pronounced – to the point that finger-like fluid bodies or ligaments are formed. Upon breakup, these ligaments look to produce a number of drops of varying size. It can also be noted that the axial distance along the jet prior to any sensible disturbances is again comparatively smaller than the previous image.

Any sensible length of jet, continuous or otherwise, is no longer observed in the fourth image. This appears to represent an operational boundary or limitation for the existence of a liquid jet. In fact, this state of the jet is often referred to as a pure atomization [24], a process where upon exiting a nozzle a volume of liquid is disintegrated and dispersed into a multitude of fine drops. Thus from any practical standpoint no jet is formed.

From the previous observations, it is clear that to characterize the surface area of a jet, an understanding of the different mechanisms behind its breakup will be quite important. Due to the variety in the states encountered by a liquid jet, disturbances exhibited upon the jet, and the forms in which the disturbances are manifested, it is also clear that quantifying the surface area will require knowledge in each of these areas. Therefore, it is appropriate to provide a review of literature relevant to the determination and dissemination of this information.

The following literature review will provide an overview of jet disintegration phenomena. Primarily chronological in structure, an historical evolution of jet disintegration research will be presented. The purpose of this approach is to display a clear, logical progression in not only the developments in this area, but also the motivations behind them.

With a cursory understanding of breakup phenomena, the various states encountered by a liquid jet will then be discussed at length. Based upon experimental and reported application information, it will be determined which states will be the most practical and relevant for analysis.

Using the information from the literature review, an approach will be developed to delimit each of the states based upon well-defined criteria. Within each delimitation, a method for characterizing the unbroken jet length, any prominent surface disturbances which lead to a sensible change in the jet surface area, as well as the size and number of the drops formed upon breakup will be proposed. This information can then be combined to provide a quantification of the surface area of a liquid jet pre- and post-breakup under a prototypical range of conditions important in the analysis of mass, momentum, and energy transport..

Chapter 2

Review of Relevant Literature

When a cylindrical liquid jet exits a circular nozzle, the jet structure is determined by the cohesive and disruptive forces acting on the jet surface. These disturbances can become amplified under favorable conditions and ultimately give rise to jet disintegration [24, 33].

Understanding these processes is important for a wide range of applications involving liquid jets. The methodologies of determining the continuous length of the jet (characterized by the growth rate of disturbances to the jet), the drop size upon jet breakup (characterized by the wave number of the most unstable disturbance), and the manner in which the jet is disrupted have been studied extensively. This chapter provides an overview of the research and analyses upon such topics as well as the basis for developing an approach for estimating the surface area of liquid jets.

2.1 General Jet Stability

The earliest documented research in the field of jet disintegration dates back over 150 years to the work of Bidone [4] and Savart [41]. Bidone focuses primarily on qualitatively describing the behavior of liquid jets issuing from nozzles of a non-circular cross section, while Savart provides what is regarded as the first quantitative data by observing the disintegration of a liquid jet in a gaseous environment.

The results of Savart are later interpreted by Plateau in his study of jet instability [32]. While Bidone and Savart are credited as the first experimentalists to study jet instability, Plateau is credited [24] as the first theoretician. He postulated that when the length of a cylindrical liquid column exceeds its perimeter, the column becomes unstable and forms two uniform, sequential drops with a total surface area less than that of the column. The work of Plateau is cited by Lord Rayleigh [33] in the publication of his more prominent theory on the stability of a liquid jet.

In his analysis [33], Rayleigh considers an inviscid, liquid jet in a vacuum. The aim of his analysis is to characterize the fastest growing disturbance on the surface of a liquid jet, as he postulates this induces breakup. Although an actual liquid jet possesses viscosity and issues into a gaseous atmosphere, the results of Rayleigh's analysis provide a reasonable first approximation of the behavior of a low speed water jets in air [43]. As most jet stability analyses build upon the foundation laid by Rayleigh, it is pertinent to present his work.

Rayleigh begins his analysis by assuming that the surface of an inviscid, liquid jet becomes disturbed upon exiting a nozzle. He characterizes the jet surface at a given time by employing a description of the jet radius.

$$r = a + f(\theta, x) \quad (2.1)$$

In Equation 2.1, r is the disturbed jet radius, a is the original jet radius, and $f(\theta, x)$ is a function describing the disturbance in terms of the angle and axial distance, which is small compared to *a.* Rayleigh applies a Fourier series expansion to the forcing term, and redescribes the radius of the jet. He continues by defining the surface energy of the jet as a quantity directly proportional to the surface area and surface tension. Comparing the disturbed and undisturbed energies, he finds the surface energy of the disturbed configuration.

$$P = \frac{\pi \sigma}{2a}\left(\gamma^2 + n_i^{\,2} - 1\right) b_n^2 \quad (2.2)$$

In Equation 2.2, P is the potential surface energy, σ is the surface tension, n_i is any positive, real integer including zero, b_n is a Fourier constant, and γ is the dimensionless wave number satisfying the relationship in Equation 2.3.

$$\gamma = k\,a = \frac{2\pi a}{\lambda} \quad (2.3)$$

The term λ in Equation 2.3 is the disturbance wavelength. By definition, γ is always positive, and as such Equation 2.2 indicates that for all values of *n* greater than unity the potential surface energy is always positive. Positive surface energy indicates stability, which is the case for nonsymmetrical disturbances; thus, a jet is stable for this type of perturbation.

Conversely, for symmetric disturbances where *n* equals zero, and when γ is less than unity, the potential surface energy is always negative, indicating instability. To ensure instability, Equation 2.4 must be satisfied - this makes γ unconditionally less than unity.

$$\lambda > 2\pi a \quad (2.4)$$

The aforementioned conditions imposed upon γ and λ provide two key insights into jet stability.

First, Rayleigh's analysis demonstrates that for non-viscous jets in a vacuum and subject only to surface tension forces, all disturbances with wavelengths exceeding the circumference of the jet will grow. Second, Rayleigh's analysis shows that the symmetric class of disturbances will grow most rapidly, and will control the breakup of jets satisfying the aforementioned criteria.

Rayleigh further recognizes that the problem of jet breakup is dynamic in nature, and combines the previous expressions to obtain the exponential growth rate at its maximum value over the interval $0 < \gamma < 1$. His result is the growth rate for the dominant or "most

dangerous" disturbance. Rayleigh postulates that it is the most dangerous disturbance that ultimately leads to jet disintegration. His expression for this quantity is given in Equation 2.6, where d_o is the undisturbed jet diameter.

$$q_{\max} = 0.97\left(\frac{\sigma}{\rho d_o^{\,3}}\right)^{0.5} \quad (2.6)$$

It should be noted that the properties in Equation 2.6 are absent of any subscripts, and refer to the liquid properties of the jet. This default convention will be adopted hereafter in the present analysis, unless otherwise stated.

Recalling Equation 2.3, the wavelength of the most dangerous disturbance is written as in Equation 2.7.

$$\lambda_{\max} = 4.51\, d_o \quad (2.7)$$

To provide a more holistic view of jet disintegration, Rayleigh continues by calculating the size of a drops following breakup. He assumes that the volume of a spherical droplet of diameter D formed in this manner is approximately equal to that contained in a cylinder of fluid, namely a portion of the jet, with diameter d_o and length 4.51 d_o.

This equality is given in Equation 2.8.

$$4.51\, d_o \times \frac{\pi}{4} d_o^{\,2} = \frac{\pi}{6} D^3 \quad (2.8)$$

Equation 2.8 is rearranged to give the droplet diameter in terms of that of the undisturbed jet. This is provided in Equation 2.9.

$$D = 1.89\, d_o \quad (2.9)$$

Thus, according to the analysis proposed by Rayleigh, a liquid jet breaks up at 4.51 times the undisturbed jet diameter and forms a spherical drop whose diameter is nearly twice that of the undisturbed jet.

Over 50 years later, Tyler obtains a similar result while analyzing the measured frequency of drop formation upon jet disintegration under conditions similar to Rayleigh's [54]. Relating the measured frequency to a disturbance wavelength, Tyler finds that the most dangerous wavelength can be expressed as given in Equation 2.10.

$$\lambda_{\max} = 4.69\, d_o \quad (2.10)$$

Using the same geometric assumptions as Rayleigh, Tyler finds an expression for the diameter of a drop formed upon jet disintegration provided in Equation 2.11.

$$D = 1.92\, d_o \quad (2.11)$$

Tyler concludes that due to the close agreement (less than 4% deviation) between his empirical relations and the analytical relations of Rayleigh, cylindrical jets breakup under the conditions required for maximum instability, as predicted by Rayleigh's theory.

Concurrent with the experiments of Tyler, Weber develops a more generalized theory for jet disintegration that includes the effects of liquid jet viscosity, velocity, and aerodynamic drag [56]. Also analyzing a jet in vacuum, Weber assumes that a jet will possess a mean flow which is subjected to symmetrical disturbances characterized by Equation 2.12.

$$f(z, r, t) = f_o(a)\, \exp(qt + ikx) \quad (2.12)$$

In Equation 2.12, f is a functional representation of a disturbance, x is the axial distance along the jet, t is the age of the jet following exit, f_o is an amplitude function, i is the square root of negative one, and all other terms retain their previous definitions.

Weber continues to obtain a characteristic equation for the exponential growth rate of the disturbance in terms of the dimensionless wave number. Though the analysis of Weber is more complex than that of Rayleigh, it retains the same overall functional form. Weber employs Rayleigh's criterion that $0 < \gamma < 1$ and finds an expression for the exponential growth rate of the most dangerous disturbance. This is given for a viscous jet in Equation 2.13.

$$q_{\max} = \left[\frac{6\mu a}{\sigma} + \left(\frac{8\rho a^3}{\sigma} \right)^{0.5} \right]^{-1} \quad (2.13)$$

For an inviscid jet, Equation 2.13 reduces to Equation 2.14.

$$q_{\max} = \left(\frac{\sigma}{8\rho a^3} \right)^{0.5} \quad (2.14)$$

Equations 2.13 and 2.14 are next used by Weber to determine the wavelength of the most dangerous disturbance, as given in Equation 2.15.

$$\lambda_{\max} = \begin{cases} 4.44\, d_o & \textit{for inviscid jets} \\ \sqrt{2}\,\pi\, d_o \left(1 + \dfrac{3\mu}{\sqrt{\rho \sigma d_o}} \right)^{0.5} & \textit{for viscous jets} \end{cases} \quad (2.15)$$

Recalling both Rayleigh's and Tyler's expressions for the most dangerous wavelength, there is little variation between their results and that of Weber in Equation 2.15 for an inviscid jet. In fact, the primary difference is attributed to approximations made in Weber's analysis based upon experimental observations [28].

Years later, Haenlein presents experimental evidence that supports Weber's theoretical analysis [14]. Haenlein uses liquids having a variety of viscosities and surface tensions, and shows that the ratio between the most dangerous wavelength and the undisturbed jet diameter is greater than that of Rayleigh's or Tyler's analyses while more agreeable with that of Weber.

In addition to quantifying the effects of viscosity on liquid jet stability, Haenlein provides qualitative evidence that suggests four distinct regions of jet disintegration [14] and is credited as the first researcher to do so [24]. He defines these regions as: drop formation without the influence of air, drop formation with minor influence of air, drop formation due to waviness of the jet, and complete disintegration of the jet. Haenlein illustrates the first three of these regions as shown in Figure 2-1.

The top image in Figure 2-1 depicts drop formation without the influence of air, as defined by Haenlein. He applies the term "varicose" to describe the surface of the jet. Haenlein also notes a linear relationship between the length of the jet prior to break up and the velocity upon exit.

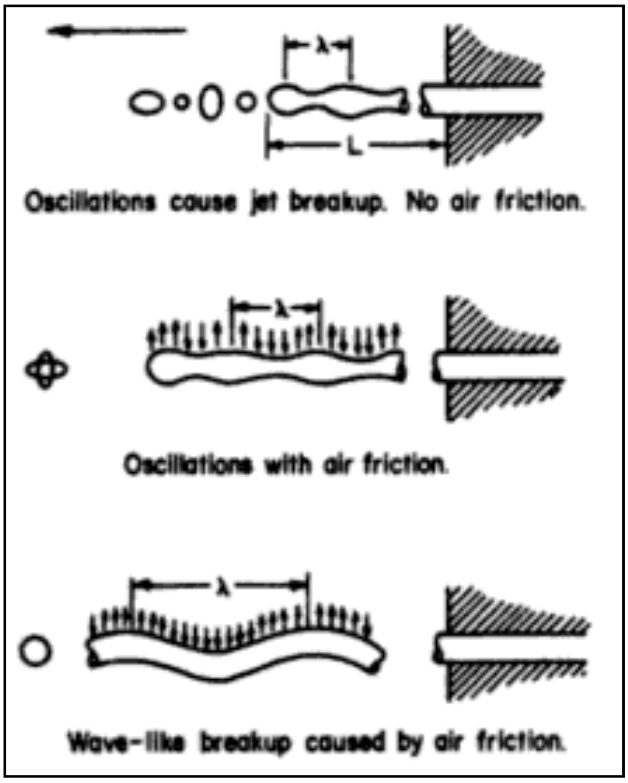

Figure 2-1: Mechanisms of drop formation [14].

The second (or middle) image in Figure 2-1 depicts drop formation with minor air influence. Haenlein notes that as the velocity of the jet is increased beyond that of the previous region, the effects of the air on the shape of the jet surface are no longer negligible. He also suggests that these effects manifest themselves by accentuating already present oscillations.

The third image in Figure 2-1 shows drop formation due to waviness of the jet. Haenlein associates this regime of jet disintegration with an observable increase in the effectiveness of aerodynamic forces in disturbing the surface of the jet. He also postulates that due to the magnitude of the aerodynamic forces present, the relative influence of surface

tension forces on jet stability becomes diminished. Haenlein applies the term "sinuous" to describe jet in this region.

Haenlein defines a fourth region of jet break up (not pictured) as complete disintegration or atomization of the jet. To elaborate, he suggests that the liquid is observed to break up at the nozzle in a chaotic manner. Although Haenlein is the first to suggest different regions or regimes of jet disintegration, texts [24, 26] suggest that Ohnesorge provides a more practical and commonly accepted classification method.

Studying photographs of jet disintegration experiments and using dimensional analysis, Ohnesorge defines a number that contrasts the viscous effects in the liquid to those of the inertia and surface tension forces [30]. The stability (or Ohnesorge) number, Oh, is given in Equation 2.16.

$$Oh = \left(\frac{\rho u^2 d_o}{\sigma} \right)^{0.5} \left(\frac{\rho u d_o}{\mu} \right)^{-1} = \frac{\mu}{(\rho \sigma d_o)^{0.5}} \quad (2.16)$$

In Equation 2.16, u is the mean jet velocity taken at the nozzle outlet and assumed to remain relatively constant over the jet length in question. As previously indicated, all fluid properties reference the liquid state. It is also important to note that these quantities represent mean or average values over the radial and axial directions for the jet length in question.

Upon closer inspection, the Ohnesorge number is a combination of two very common numbers in nuclear engineering, the Weber and Reynolds numbers, respectively. In the interest of review, it is pertinent to mention that the Weber number relates the inertial forces in a fluid to the surface tension, whereas the Reynolds number provides a measure of the inertial forces in a liquid with respect to the fluid viscosity.

In his book [24], Lefebvre provides a good depiction of the disintegration regimes according to Ohnesorge; this is given in Figure 2-2.

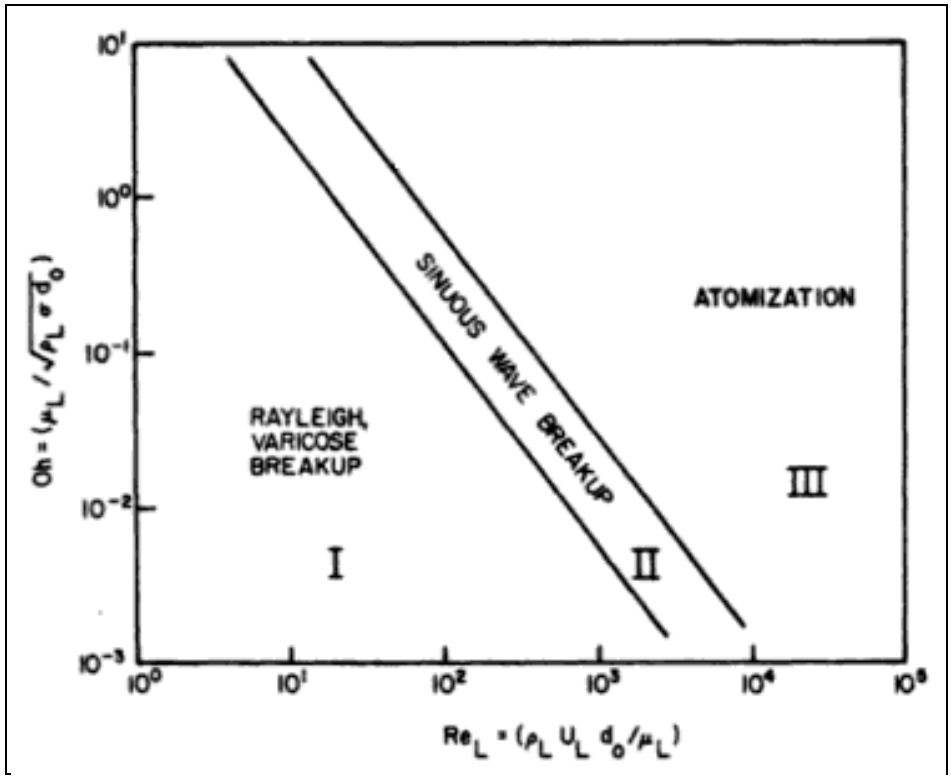

Figure 2-2: Classification of breakup modes according to Ohnesorge [24].

From Figure 2-2, it is implied that low Reynolds number jets possess a varicose structure and disintegrate in a manner consistent with that described by Rayleigh. Such behavior is characterized by region I. Ohnesorge observes that in this region, jets break up into large, uniformly-sized drops [30].

At intermediate Reynolds numbers, indicated by region II in Figure 2-2, the disintegration of the jet is said to be due to oscillations with respect to the central axis of the jet which make it appear twisted [30]. Ohnesorge observes that the magnitude of these perturbations increases with air friction on the jet surface until it completely disintegrates. For this region, a range of drop sizes is produced [30].

Region III is characteristic of high Reynolds number jet flows. In this region, complete atomization is typically observed almost immediately upon discharging from the nozzle [30]. A contemporary researcher of Ohnesorge, Castleman suggests that, for region III, the most important factor in the process of jet disintegration is relative motion between the outermost layer of the jet and the air surrounding it [5]. Castelman's conjectures are based upon his work as well as that of previous researchers [9, 40].

Disturbances created by this interaction give rise to irregularities on the jet surface. These irregularities are observed to first produce waves and wave-like structures, then unstable ligaments or fingers of liquid. Though their mean velocities are observed to be approximately that of the jet, waves and ligaments can possess different shapes and

orientations [21, 58]. After some distance, the waves and/or ligaments disintegrate to produce smaller drops.

Overall, drawing upon the results of Haenlein [14] as well as his own, Ohnesorge asserts that regardless of the noted difference in the appearance and disintegration modes characteristic of each regime, the boundaries and transitions between them are not so well defined. The lines shown in Figure 2-2, barring that of Meisse, represent the best empirical fit to the jet disintegration data available at the time of Ohnesorge's experiments.

Building upon the ideas of Ohnesorge, Meisse [29] states that experimental jet disintegration data is more accurately described when an additional line or break up regime is added, as shown in Figure 2-2. Similar to that of his contemporaries, the work of Meisse is primarily empirical in nature.

More recently in his dissertation, Reitz [35] compiles the work of a number of noted researchers in jets [14, 30] and diesel sprays [29, 40] as well as that of his own and proposes four regimes of jet disintegration that can be encountered. The regimes described by Reitz are currently regarded [11] as the best description of the modes of jet breakup phenomena. These regimes are illustrated in Figure 2-3.

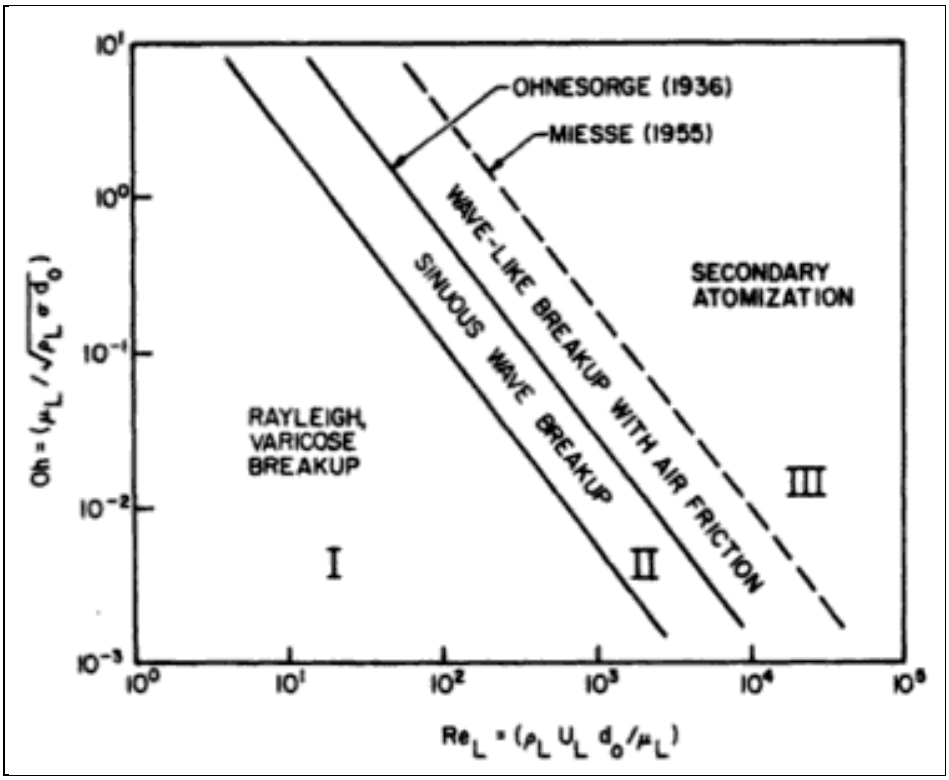

Figure 2-3: Jet disintegration regimes according to Ohnesorge and Meisse [24].

In addition to a graphical representation of the jet breakup regimes, Reitz develops accepted [11, 24, 26] criteria for the determination of the breakup mode to be encountered. Again, this is based upon a variety of experimental data in the area. The criteria developed by Reitz are listed in Table 2-1.

Similar to Meisse, Reitz finds that four regions are necessary to fully describe jet disintegration. As each regime possesses different geometries and breakup mechanisms, they are discussed individually in the following sections.

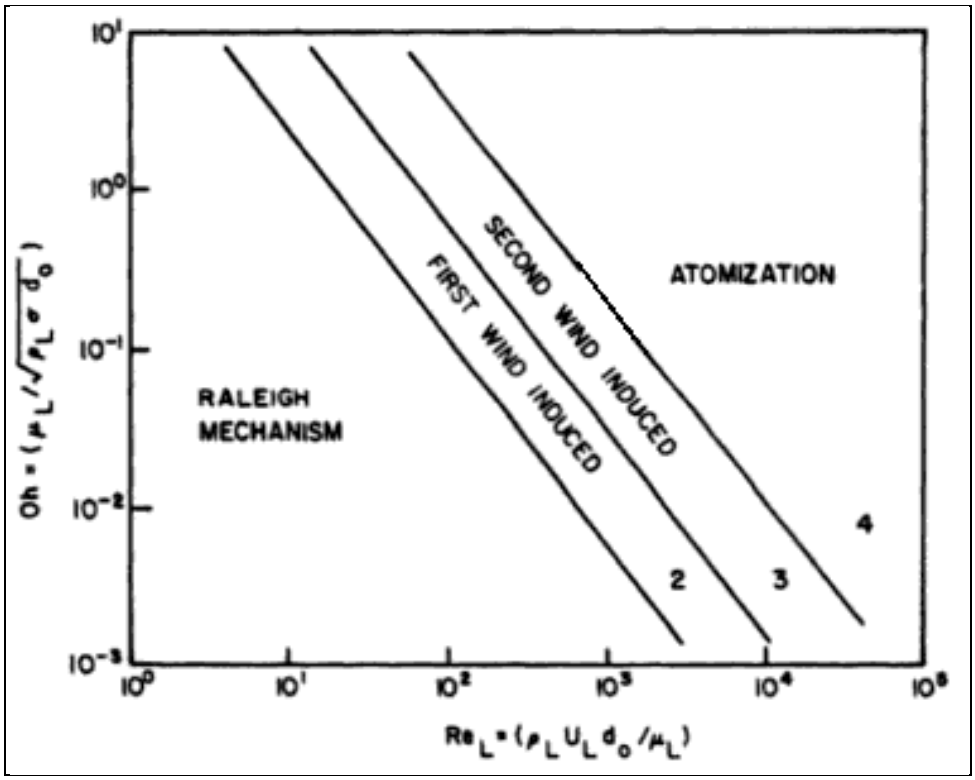

Figure 2-4: Modes of jet disintegration [24].

Table 2-1: Classification of jet breakup regimes [36].

Regime No.	Description	Predominant Drop Formation Mechanism	Regime Transition
1	Rayleigh Breakup	Surface Tension	$We_A > 0.4$ or $We_A > 1.2 + 3.4\ Oh^{0.9}$
2	First Wind-Induced Breakup	Surface Tension & Air Friction	$We_A > 13$
3	Second Wind-Induced Breakup	Air Friction & Opposition by Surface Tension	$We_A > 40.3$
4	Pure Atomization	Multiple - Single Cause Unknown	-

2.2 Jet Disintegration Modes

Reitz [35] and subsequently Reitz and Bracco [34] discuss the various mechanisms associated with the breakup of liquid jets. In most applications, there is no clearly-defined demarcation between these regimes. Though various mechanisms and hypotheses have been suggested, no single mechanism is considered responsible for all jet breakup processes; rather, a combination of factors is postulated to be involved.

Regardless of the mechanisms, jet disintegration is classified into four primary modes or regimes, as previously discussed. A fifth regime, liquid dripping, is also described by researchers [11, 26] as the most elementary mode of liquid jet/drop formation. To be complete, all five regimes are pictured in Figure 2-5 and are discussed in this section.

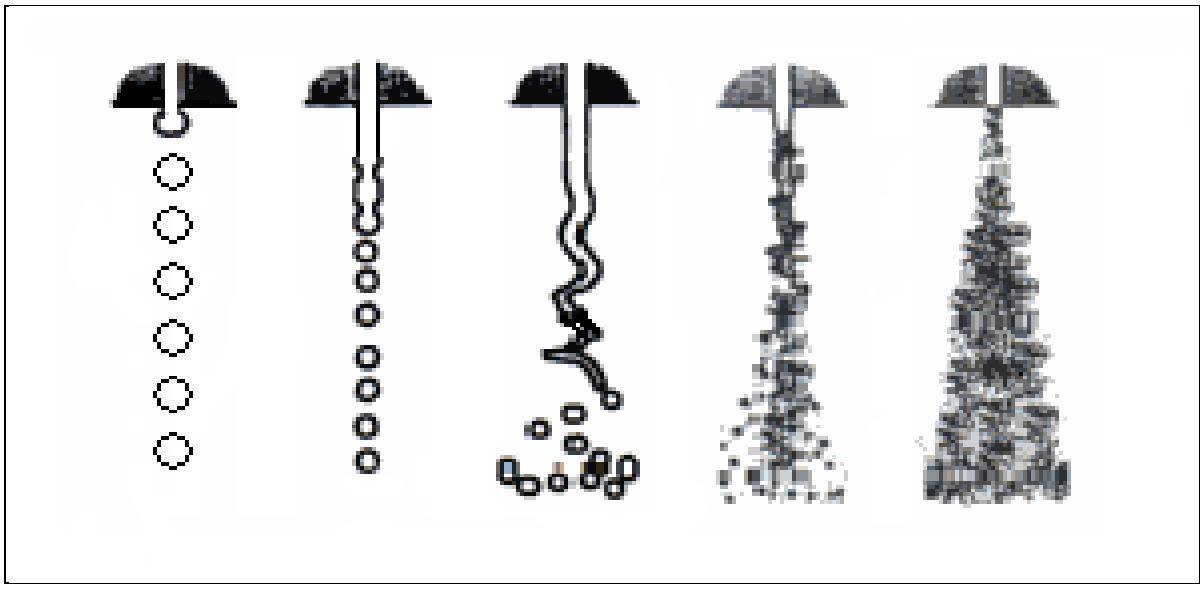

Figure 2-5: Illustration of jet disintegration modes [26].

Progressing from left-to-right in Figure 2-5, one encounters the liquid dripping, Rayleigh, first wind-induced, second wind-induced, and atomization breakup regimes as described by Reitz [35] and Liu [26].

2.2.1 Liquid Dripping

The liquid dripping regime is the most basic mode of liquid jet/drop formation. This regime is characterized by very low flow rates and large drops of very uniform size being formed. In extreme cases of liquid dripping, drops can be suspended from thin, capillary-like tubes of liquid – which lends this regime to be categorized as a corollary mode of jet disintegration [26].

In this region, liquid issuing from an orifice or nozzle forms a hanging or pendant drop under the action of gravity. This collection of liquid remains stationary and grows in size until the gravity force on the liquid exceeds the surface tension force. At this point, the liquid detaches to form a spherically-shaped drop. The size of the drop formed is determined exclusively by the competing gravitational and surface tension forces, as the flow velocities for this mechanism are low.

Tanasawa and Toyoda [51] study the liquid dripping mechanism in greater detail. They find that various forms of suspended drops can be obtained for different radii of curvature at the drop tip. These researchers also present data for a number of different

dripping situations including orifice discharge, detachment from a cylindrical tube, detachment from a plane surface, and formation and detachment on the tip of an electrode. Suffice to say that this mechanism is not an effective means of jet production for any of the practical applications previously discussed. This regime is typically not observed in any practical application [26].

2.2.2 Rayleigh Breakup

When the flow rate of a liquid through and orifice or nozzle exceeds a given value, equilibrium is no longer maintained between the surface tension and gravitational forces acting thereon. At this point, a transition from liquid dripping to the formation of a liquid jet takes place [26].

Rayleigh [33] finds it prudent to characterize the continuous length of the jet prior to breakup and the size of the drops formed upon breakup as these parameters govern the growth rate and wavelength of the most dangerous disturbance. Expressions for these values are presented previously in this chapter. A photographic example of this mode of breakup is given in Figure 2-6.

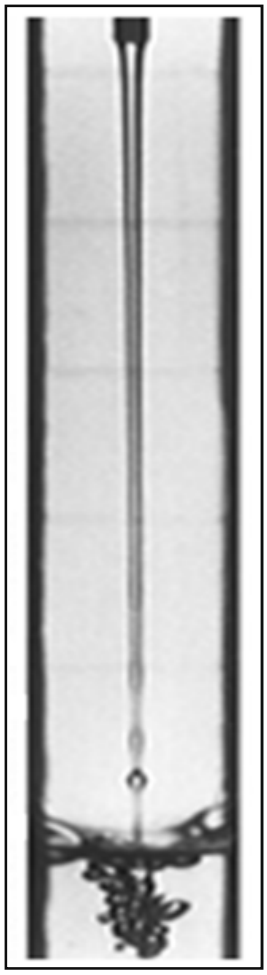

Figure 2-6: Jet disintegration example in the Rayleigh regime [21].

The observations of a number of researchers [24, 35] conclude that in this disintegration mode, liquid jet breakup and subsequent drop formation are fairly regular and predicable in nature. The phrase varicose breakup is sometimes used to describe this region [28], as the jet is observed to elongate and thin, or pinch, immediately prior to breakup. This phenomenon is shown in Figure 2-6.

In the Rayleigh breakup regime, jet disintegration is caused by growing axisymmetric oscillations of the jet surface. These oscillations are the result of interactions between the inertial force which delays breakup and the surface tension force which acts to disrupt the jet; aerodynamic effects are negligible due to the low velocity of the jet. The analyses of Rayleigh and Weber suggest, and more recently Reitz confirms experimentally that the continuous length of the jet is linearly proportional to the jet velocity and that the diameters of the drops formed are nearly uniform in size and larger than that of the undisturbed jet.

2.2.3 First Wind-Induced Breakup

Upon increasing the velocity of a jet beyond that characteristic of the Rayleigh regime, the effect of aerodynamic forces on the stability of the jet becomes relevant [14]; and it enters the first wind-induced (FWI) breakup regime. As the Weber number of a jet is increased, air resistance becomes more prevalent due a higher relative velocity between the jet and the surrounding air. While the surface tension of the jet continues to induce wave growth, inertia and air resistance tend to oppose it [35].

Disintegration of the jet is due to the growth of oscillations with respect to the jet axis. These oscillations produce sinuous, unstable surface waves which distort the mean jet flow in the cross-flow direction, giving rise to wavy perturbations, and in some cases, finger- or ligament-like segments. Once pronounces waves and/or ligaments are produced, air resistance no longer acts as a damp for instability. Both waves and ligaments ultimately

breakup to produce one or more drops of varying size. Figure 2-7 provides a photograph of these phenomena.

Figure 2-7: Jet disintegration example in the FWI [21].

Continuing with Rayleigh's characterization, it can be said that jets in the FWI regime experience liquid distortion several nozzle diameters downstream of the discharge nozzle exit. This distortion can either lead directly to breakup or to a transitional region exhibiting prominent waves and/or ligaments. Further, the average diameters of droplets formed are

smaller than the jet diameter. Literature [26] suggests that a distribution be used to describe the variation of droplet size; however, this will be discussed later in this chapter.

2.2.4 Second Wind-Induced Breakup

Increasing the jet velocity beyond that of the first wind-induced regime, the breakup of the jet is found to be caused by the growth of unstable, shorter-wavelength disturbances on the surface of the jet. These waves arise due to the relative motion between the jet and the surrounding air [28]. In this regime, the second wind-induced (SWI) breakup regime, air resistance no longer acts to damp out surface disturbances along the continuous jet. Rather, its magnitude exceeds that of the surface tension, such that disturbances become the predominant cause of jet disintegration.

An increase in the Weber number of the jet results in a decrease in the maximum growth rate and corresponding wavelength of sinuous surface waves. However, both the maximum growth rate and most dangerous wavelength become independent of the jet diameter at sufficiently high Weber number values [35]. Oscillations continue to distort the mean jet flow in the cross-flow direction, giving rise to finger- or ligament-like segments. This occurs in a fewer number of nozzle diameters downstream of the exit and the magnitude of the distortions in the cross-stream direction is much greater than in the previous regime. Figure 2-8 provides a photograph of these phenomena.

Figure 2-8: Jet disintegration examples in the SWI regime [21].

Liquid jets in the SWI regime experience distortion only few nozzle diameters downstream of the discharge nozzle exit. Further, the average diameters of droplets formed are smaller than the jet diameter, but exhibit a less uniform range of sizes than those of the FWI regime. Literature again suggests that a distribution be used to describe the variation of droplet size [26].

2.2.5 Pure Atomization

At extremely high velocities, complete disintegration of the jet occurs within a very short length from the nozzle exit. Breakup occurs in a highly chaotic and irregular manner, and a spray is formed. This process is called atomization, which also describes the breakup of jets in this regime. Figure 2-9 provides a photograph of a jet atomizing within approximately three nozzle diameters from the exit.

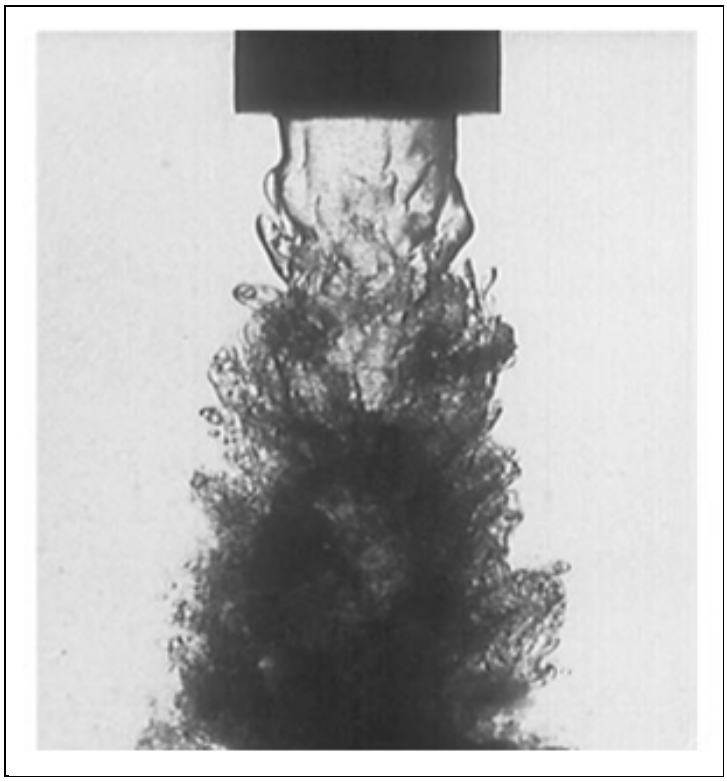

Figure 2-9: Jet disintegration example in the atomization regime [21].

In the atomization regime, a single, predominant breakup mechanism is not defined in the literature. Most authors suggest that disintegration occurs due to a combination of disturbances and perturbations [14]. As with the other regimes, irregularities are found in the originally smooth liquid jet surface leading to unstable wave growth. However, this growth occurs in a much more rapid manner.

Similar to the wind-induced regimes, perturbations of the jet surface produce unstable ligaments. Like the disturbances that produce them, the ligaments form and disintegrate in a much more rapid manner than in previous regimes. Even further, much smaller droplets are generated upon the disruption of the ligaments [35]. Drop sizes are spread over a wider range, where the average diameters are much smaller than the jet [29].

2.3 Influence of Turbulence on Jet Stability

As discussed in the previous sections, jet disintegration is caused by a number of effects which are commonly categorized into modes or regimes of breakup. However, another set of considerations exists with regard to the breakup of jets – the turbulent nature of the jet flow. Chigier [7] provides a comprehensive listing of triggering mechanisms for the initiation of liquid surface disturbances.

He asserts that the major contributors are: pulsations in supply lines to the nozzle, sharp edges within the nozzle causing separated flows, wall surface roughness within the nozzle, internal turbulence generation and cavitation prior to and following exit, competition between the surface tension and jet flow characteristics, and interaction of liquid surface with surround air flows downstream of the exit [7]. Since most of these factors are directly related to either the treatment or generation of turbulence, this list suggests its importance in jet disintegration.

Schweitzer [43] provides an excellent qualitative description of hydraulic turbulence in jets. He asserts that a jet emerges from a nozzle in either a laminar or turbulent state and that this state is both dependent upon the flow upstream of the nozzle and perpetuated along the continuous length of the jet. When the liquid particles travel primarily in the stream-wise direction the flow is laminar, whereas the crossing of liquid particle paths to cross-stream velocity components is indicative of turbulent flow.

Tanasawa and Toyoda [51] found turbulence important enough to devise their interpretation of jet breakup with respect to laminar, transition, turbulent, and spray jet flows. Noting the different appearances of the jet surface for each type, they suggest that disintegration is aided by internal motions in the flow.

For laminar flows, a smooth, cylindrical liquid is observed to possess bead-like swelling and contraction, accompanied by rotationally symmetrical oscillations of the liquid surface as disturbances arise. This beading occurs at the tip of the liquid column primarily due to the growth of surface instabilities [49].

For turbulent flows, lateral oscillations are observed as early as discharge from the nozzle. Sinuous perturbations of the jet arise and vary greatly in size and shape with escalating Reynolds numbers. They travel in the stream-wise direction of the jet to the tip of the liquid column and form readily observable waves throughout their proliferation. The waviness due to the turbulence is subsequently amplified by air resistance on the surface of the jet as disturbances increase in magnitude [31, 51].

Tanasawa and Toyoda [51] note that with very high Reynolds numbers, the wavy liquid surface may be dragged by the surrounding air and drawn out into increasingly smaller ligaments or narrow, leaf-like membranes. These ligaments are orders of magnitude smaller than the jet or wave diameters. They are quickly detached from the jet by the rapid growth of dents in their surface due to interaction with a gaseous environment and are observed to breakup swiftly into several very small droplets [38].

2.3.1 Jet Stability Curve

Similar in concept to the methods presented by Reitz, researchers also characterize the stability of jets by experimentally determining the relationship between jet velocity and breakup (or continuous) length. First proposed by Smith and Moss, a length-velocity or stability curve provides this information [48]. Lefebvre provides qualitative visualization of the stability curve in his text [24]. This is provided in Figure 2-10.

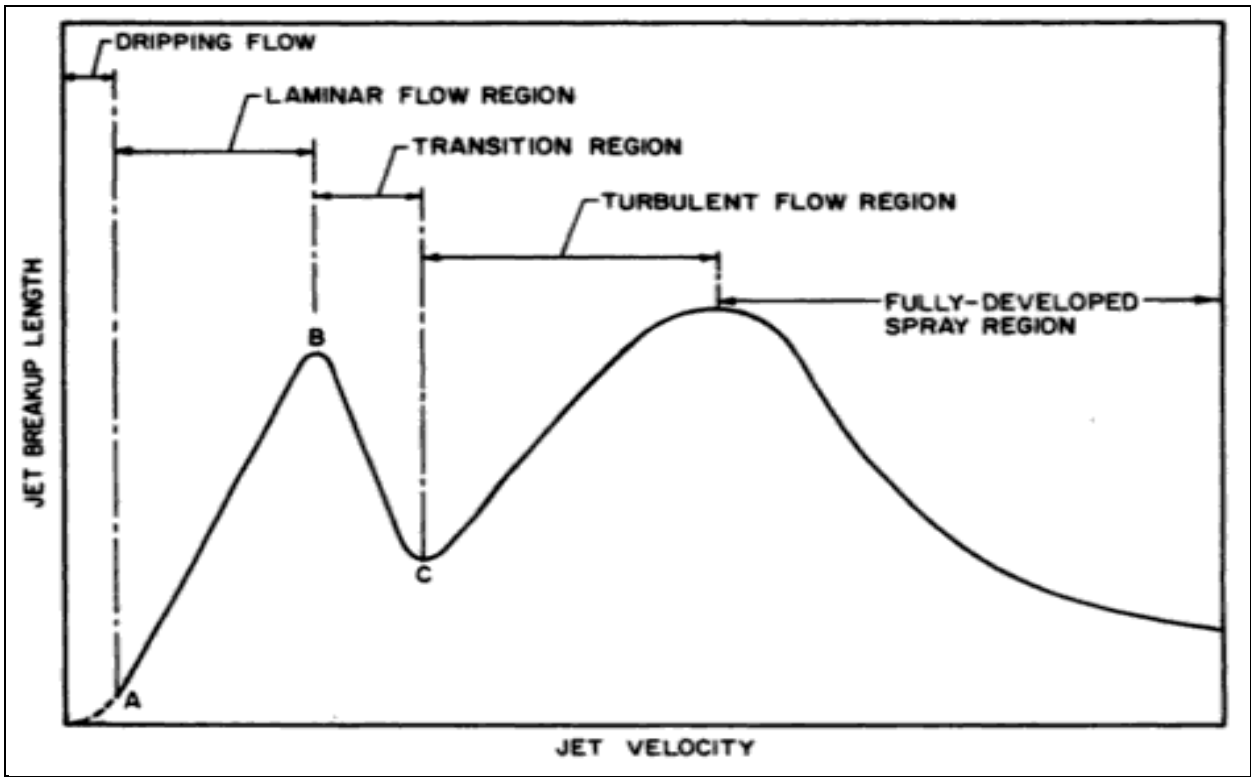

Figure 2-9: Illustration of jet stability with regard to velocity [24].

The stability curve partitions the modes of jet breakup into distinct regimes. Each of the regimes, from dripping flow to that of a full-on spray, is labeled in Figure 2-10. Though these regimes are analogous to those of Reitz, there is not a one-to-one correspondence,

especially on a quantitative basis [26]. That said, researchers such as Grant and Middleman, Schiller, and Van de Sande and Smith have proposed expressions for a critical Reynolds number, below which any disturbances in the flow will damp out. This Reynolds number is represented by point B, in Figure 2-10.

According to Grant and Middleman, this point corresponds to a change in the breakup mode from varicose to sinuous [13]. Schiller proposes a value of 2,320 for the critical Reynolds number [42]. With a great deal more experimental data, Grant and Middleman later propose the empirical expression in Equation 2.17.

$$\mathrm{Re}_{crit} = 3.25\,Oh^{-0.28} \qquad (2.17)$$

Van de Sande and Smith also propose an expression for the transition from laminar to turbulent jet flow [55]. However, instead of characterizing the point where a purely laminar jet ends, they focus on capturing the beginning of the transition from a laminar to turbulent jet. Their expression is provided in Equation 2.18.

$$\mathrm{Re}_{crit} = 12{,}000\left(\frac{x}{d}\right)^{-0.3} \qquad (2.18)$$

2.3.2 Laminar Jet Disintegration

In Figure 2-9, the AB or laminar portion of the curve corresponds to a mode jet disintegration resulting from the disturbances described by Rayleigh and Weber. Weber's analysis shows that a small axisymmetric disturbance grows at an exponential growth rate until it reaches amplitude on the order of the jet diameter. This can be used to calculate t_b, the time required for jet breakup as given in [24] and shown in Equation 2.19.

$$t_b = \frac{\ln\left(d_o \big/ 2f\right)}{q_{\max}} \quad (2.19)$$

In Equation 2.19, f refers to a function describing the surface instabilities whose magnitude is experimentally determined. Lefebvre alternatively defines the time in terms of the continuous jet length, l_b, and the jet velocity in Equation 2.20 [24].

$$t_b = \frac{l_b}{u} \quad (2.20)$$

Combining Equations 2.19 and 2.20 with the results of a Rayleigh's stability analysis for an inviscid jet given in Equation 2.6, one finds an expression describing the continuous length of a laminar jet.

This expression is provided in Equation 2.21, where $\left(\frac{d_o}{2f}\right)$ is the value of the initial disturbance.

$$l_b = 1.03 d_o We^{0.5} \ln\left(\frac{d_o}{2f}\right) \quad (2.21)$$

Using the results of Weber's stability analysis on a viscous jet given in Equation 2.13, one finds the expression describing the continuous length of a laminar, viscous jet. This is given in Equation 2.22.

$$l_b = d_o We^{0.5} (1 + 3Oh) \ln\left(\frac{d_o}{2f}\right) \quad (2.22)$$

Comparing Equations 2.21 and 2.22, two conclusions quickly emerge. First, the effects of viscosity on the continuous length of a jet are immediately apparent as this value is proportional to $d_o^{1.5}$ for inviscid jets and d_o for viscous jets. This implies the relative importance of considering viscosity in a jet stability analysis. Second, for any practical application of either equation the value of the initial disturbance, $\left(\frac{d_o}{2f}\right)$, must be determined. Grant and Middleman and other researchers [24, 53] are quick to point out that this cannot be determined a priori.

Sterling and Sleicher show that discrepancies exist in Weber's theory due to the absence of velocity profile relaxation [49]. Mahoney and Sterling expound upon this concept and present an equation for the continuous length of laminar jets [27]. This expression is given in Equation 2.23.

$$l_b = \frac{d_o We^{0.5}(1+3Oh)\ln\left(\frac{d}{2f}\right)}{f(Oh,We)} \quad (2.23)$$

Equation 2.23 is nearly identical to Equation 2.22 except that a function of the Ohnesorge and Weber numbers is added to the denominator to account for velocity profile relaxation. Mahoney and Sterling suggest a number of expressions for predicting this function [27], but they are not listed here to their complexity and limited applicability.

To demonstrate the success of their expression in predicting the breakup length, Mahoney and Sterling [27] provide several comparisons with predictions based upon Weber's results, their expression, and experimental data. Lefebvre includes one such plot in his text, which is provided in Figure 2-11.

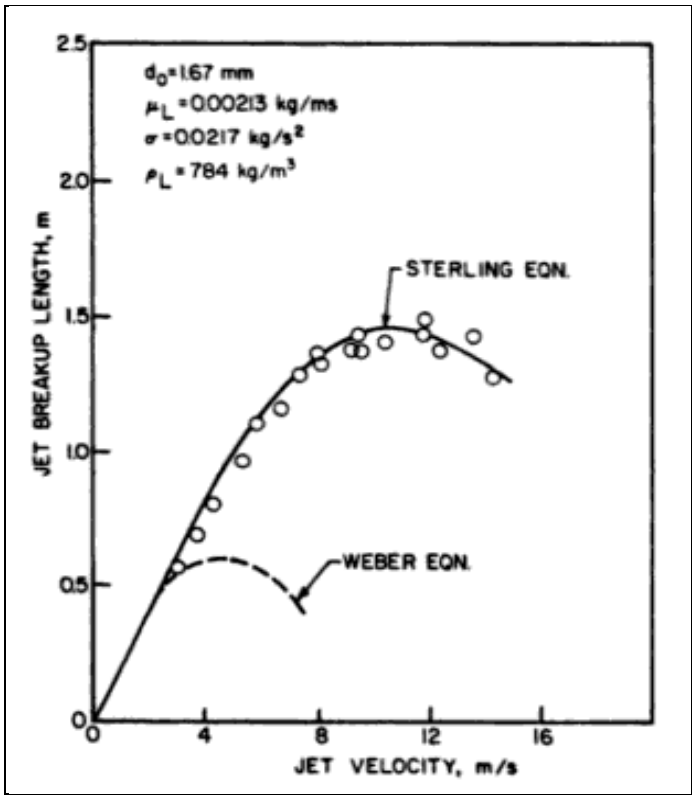

Figure 2-11: Comparison of experimental data with analytical predictions using the results of Weber and Mahoney and Sterling [24].

It is apparent from Figure 2-11, as well as the other results provided by Mahoney and Sterling that an improvement to Weber's original analysis is greatly beneficial when applied to predicting the breakup length of jets.

Grant and Middleman later collect and extensive amount of experimental data and propose a simple yet robust correlation that accounts for the considerations of the aforementioned analyses [13]. This correlation is reported to yield good agreement (well

within an order of magnitude) with data in the laminar region [11, 39], and is given in Equation 2.23.

$$l_b = 19.5 d_o We^{0.5} \left(1 + 3Oh\right)^{0.85} \quad (2.23)$$

2.3.3 Turbulent Jet Disintegration

Though many researchers stress the importance of aerodynamic effects on jet stability of jets and disintegration, many disagree with the hypothesis of Castleman [5] that suggests these effects are always dominant beyond the Rayleigh regime. Early disagreements with this idea in the literature arise from a series of high speed photographs taken by Hoyt and Taylor [17]. One such photograph, an enlarged view immediately downstream of a discharge nozzle, is provided in Figure 2-12.

The photographs of Hoyt and Taylor are later referenced by Reitz and Bracco, who draw attention to the fact that for turbulent jets, the undisturbed jet length can be up to an order of magnitude smaller than the jet diameter [34]. This suggests that the previously discusses analyses (for laminar jets) are not completely valid in the presence of turbulence, as their theory is based solely upon the propagation of disturbance along a smooth, continuous jet surface.

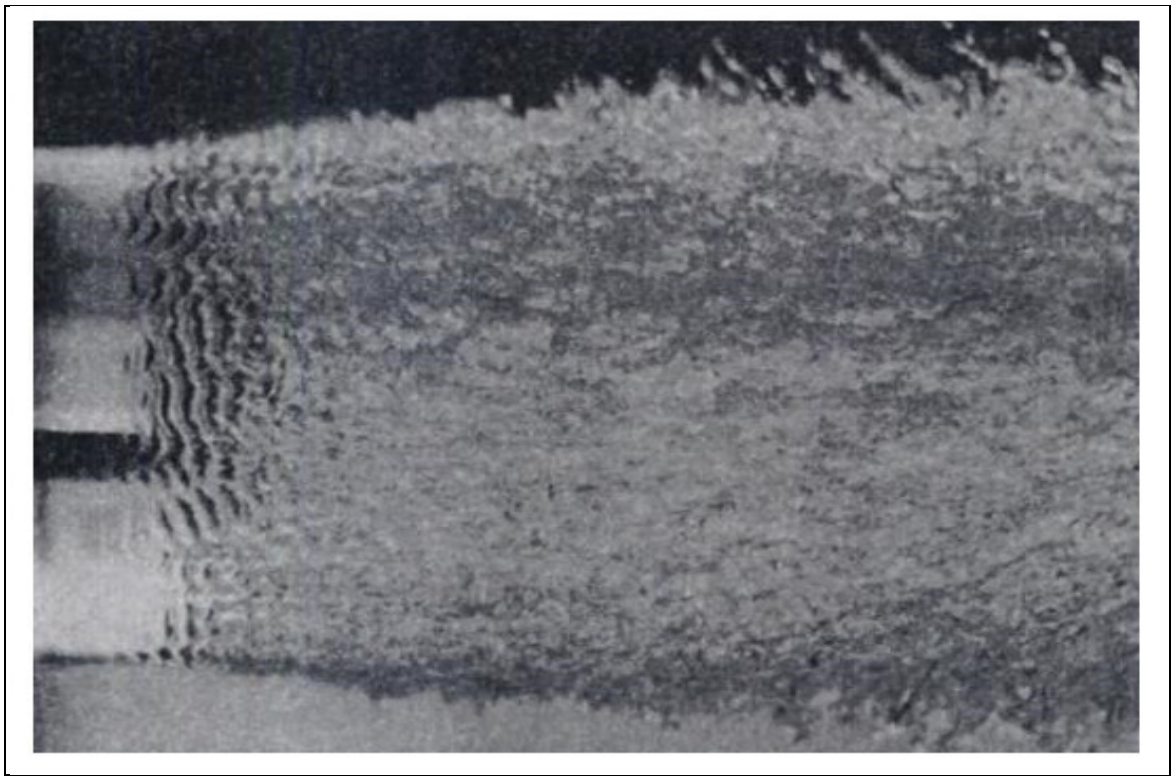

Figure 2-12: Enlarged view of a turbulent water jet [24].

Researchers have proposed a variety of theories for the mechanism(s) behind turbulent jet disintegration. This chapter already mentions Schweitzer's [43] assertion that turbulence due to flow upstream of the nozzle leads to breakup. Bergwerk [2], DeJuhasz [9], and Sadek [37] suggest that turbulence generated within the discharge nozzle alone leads to breakup, although they disagree on the point where breakup actually begins. Eisenklam and Hooper [12] propose that the relaxation of the jet velocity profile is the dominant mechanism behind the disintegration of both laminar and turbulent jets.

Conversely, the research of Reitz & Bracco states that there is no single cause responsible for breakup, especially in the case of turbulent jets [34]. They imply that jet disintegration is far too complex to be attributed to a single mechanism, and as such is caused by a combination of the aforementioned phenomena.

Due to this complicated nature of turbulent disintegration, the only practical means available for predicting the continuous length of a turbulent jet lies in empirical correlations. One such correlation is the result of some of the earliest, well-regarded work with turbulent jets by Meisse, a combustion researcher. Meisse obtained turbulent jet disintegration data for a number of fluids under a variety of conditions [29]. Lefebvre provides a correlation of Meisse's water data in his text [24], which is given in Equation 2.24.

$$l_b = 538 d_o We^{0.5} \mathrm{Re}^{-0.625} \quad (2.24)$$

Following Meisse, the previously discussed jet disintegration experiments of Grant and Middleman lead to the development of an empirical correlation for the breakup length of turbulent jets. This expression, given in Equation 2.25, is regarded by texts [24, 26] as the best-agreeing correlation for the entire range of turbulent jet disintegration.

$$l_b = 8.51\, d_o We^{0.32} \quad (2.25)$$

More recently, Sallam et al. provide further research upon turbulent jet disintegration, which suggests that a segmented approach to correlating the continuous jet length is more accurate [39]. Figure 2-13, illustrates the ability of their correlations as well as that of Grant and Middleman to predict experimental data from a number of researchers.

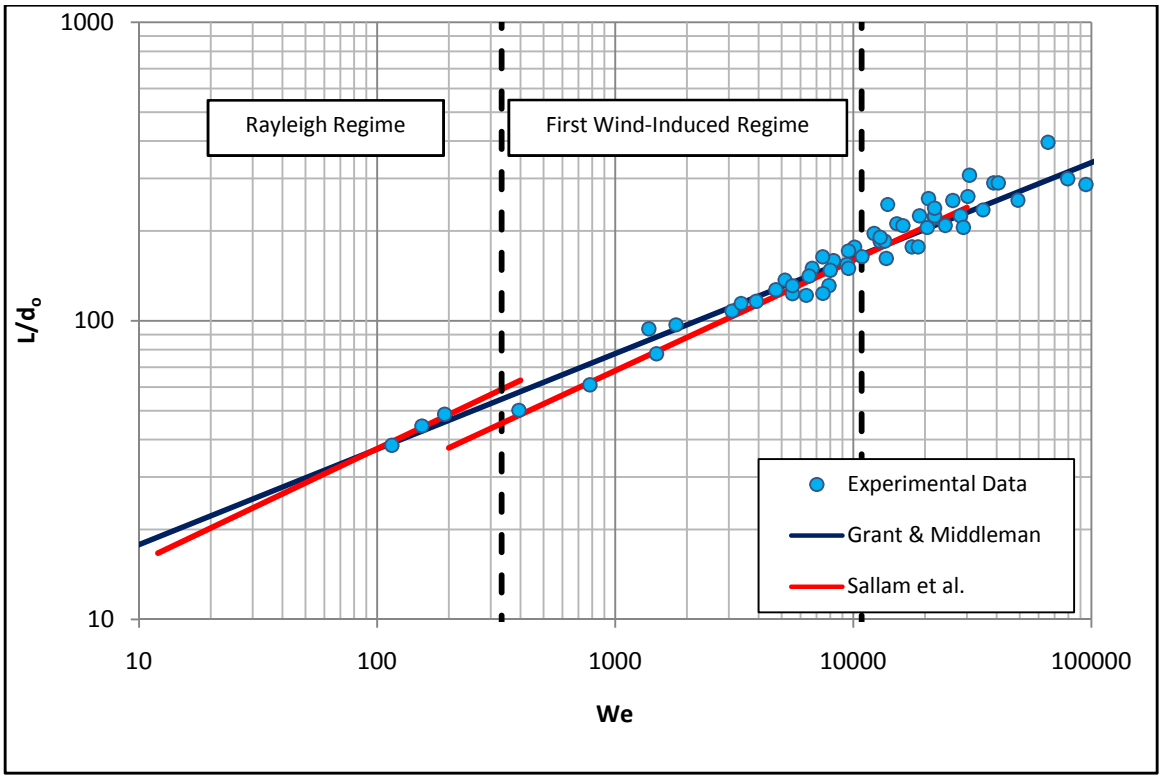

Figure 2-13: Mean liquid column breakup lengths of turbulent round jets [39].

It is immediately apparent from Figure 2-12 that the piecewise correlations proposed by Sallam et al. yield a better agreement with turbulent jet experimental data both locally in the Rayleigh and FWI regimes and overall the full range of conditions studied.

In the Rayleigh regime, the correlation suggested by Sallam et al. for turbulent jets [39] is given as Equation 2.26.

$$l_b = 5.0 d_o We^{0.5} \quad (2.26)$$

In the wind-induced regimes, the correlation suggested by Sallam et al. for turbulent jets [39] is given as Equation 2.27.

$$l_b = 2.1 d_o We^{0.5} \quad (2.27)$$

2.4 Post-Breakup Jet

To this point of the chapter, literature is presented regarding the continuous region of liquid jets. In addition to the solid jet, researchers also study the post-breakup or broken jet. The treatment of this region dates back to Rayleigh's analysis, where he calculates the diameter of drops produced upon jet disintegration. Different regimes or modes are proposed to characterize unbroken jets (excluding liquid dripping), and are also used for broken jets.

Logically, as these regimes are defined by the primary breakup mechanism, they are also directly related to the size, shape, and quantity of drops produced. Literature provides treatments for drop production by jet disintegration in these breakup regimes, and the following sections review them on an individual basis.

2.4.1 Rayleigh Mode Broken Jet

Jets breaking up in the Rayleigh mode do so as a result of growing axisymmetric oscillation on the jet surface. These oscillations are caused by instability between the surface tension and inertial forces acting on the jet. Classical treatments of this instability have been found to be effective in determining the continuous length of the jet as well as the size of the drops produced upon breakup [24, 26].

Rayleigh and Tyler present simple, straightforward methods for determining the drop size based upon a disintegrating cylinder of liquid characterized by the most dangerous wavelength and the undisturbed jet diameter. Each of the results, given in Equations 2.9 and 2.11 respectively, applies an empirical coefficient to the undisturbed jet diameter to determine the drop diameter. It is important to note, though, that the assumption of a single drop formation following breakup is quite valid throughout the regime, as the Rayleigh breakup regime is very ordered and predictable [28].

Using an instability analysis in conjunction with Rayleigh's instability theory, Teng et al. propose that the mean diameter of drops produced is related the Ohnesorge number [52]. Their expression for the drop diameter is provided in Equation 2.28.

$$D = d_o \left(\frac{3\pi}{\sqrt{2}} \right)^{1/3} \left(1 + 3Oh\right)^{1/6} \quad (2.28)$$

Teng et al. note that although there is some variation of drop size in the Rayleigh regime, it is minor and can often be neglected [24]. They provide experimental drop diameter information from their research and that of others to demonstrate the accuracy of their correlation, which is within 5% for the entire range of data

2.4.2 Wind-Induced Broken Jet

Increasing the Reynolds number of the jet, the wind-induced breakup regimes are encountered. These modes of breakup are characterized by drops varying much more in size than those of the Rayleigh regime, and result in the production of more than one drop upon disintegration [26]. Due to the variation in drop sizes, it becomes convenient to discuss the size of the drops with a distribution function as opposed to an average value.

As with many naturally-occurring particle distributions, drop sizes are most often described using a log-normal distribution [26]. Doing so suggests that the distribution will be normal or Gaussian in nature and that the logarithm of the drop diameter can be used as the variable. The governing function for a log-normal distribution is given in Equation 2.29.

$$\frac{dN}{dD} = \frac{1}{\sqrt{2\pi}\, D\, s_g} \exp\left[-\frac{1}{2{s_g}^2} \ln\left(\frac{D}{\overline{D}_n} \right)^2 \right] \quad (2.29)$$

In Equation 2.29, N is the number of drops of a given diameter D, D_n is the number geometric mean drop size, and s_g is the standard deviation of D from the mean value D_n. The number geometric mean drop size can be written for a surface as in Equation 2.30 and also for a volume as in Equation 2.31.

$$\overline{D}_2 = \left[\frac{\int_{D_{\min}}^{D_{\max}} \left(D^2 \frac{dN}{dD} \right) dD}{\int_{D_{\min}}^{D_{\max}} \left(\frac{dN}{dD} \right) dD} \right] \quad (2.30)$$

$$\overline{D}_3 = \left[\frac{\int_{D_{\min}}^{D_{\max}} \left(D^3 \frac{dN}{dD} \right) dD}{\int_{D_{\min}}^{D_{\max}} \left(\frac{dN}{dD} \right) dD} \right] \quad (2.31)$$

For heat and mass transfer applications, it is extremely important to properly characterize the drop diameter. As such, most researchers suggest the combination of Equations 2.30 and 2.31 into a term called the Sauter Mean Diameter (SMD). Expressions for drop diameters following jet disintegration are typically given in terms of the SMD. Equation 2.32 mathematically describes the SMD upon combination and simplification.

$$d_{smd} = \frac{\sum_i N_i D_i^3}{\sum_i N_i D_i^2} \quad (2.32)$$

A number of researchers have provided correlations of drop diameter data for jets in these regimes. Harmon [15] is one of the earliest available SMD correlations for jet disintegration taking into account aerodynamic effects. His expression for the SMD of drops upon breakup, a fit of Meisse's water jet data, is given in Equation 2.33.

$$d_{smd} = 3330\left(d_o^{\,0.3}\mu_l^{\,0.07}\rho_l^{\,-0.648}\sigma^{-0.15}\,u^{-0.55}\mu_g^{\,0.78}\rho_g^{\,-0.052}\right) \quad (2.36)$$

More recently, Wu et al. and Wu and Faeth have studied turbulent jets under a wide range of Weber numbers. They assume that the SMD is proportional to the turbulence in the flow, surface tension instabilities present, and the aerodynamic interaction between the jet surface and a gaseous environment [57, 58]. Dumouchel reports satisfactory agreement of Wu et al.'s correlation with experimental data [11], as written in Equation 2.34.

$$d_{smd} = \frac{7\,d_o}{We_g}\left[\left(\frac{x}{d_o}\right)^{0.5}\frac{We_g}{\mathrm{Re}_l^{\,0.5}}\right]^{0.87} \quad (2.34)$$

The term x in Equation 2.34 is the streamwise distance from the issuing nozzle exit.

2.4.3 Pure Atomization Broken Jet

The primary atomization regime is by far the most chaotic and least understood of the jet disintegration regimes. As such, there are no practical, theoretical analyses or models provided in the literature [11, 26]. All expressions for the SMD of drops in this regime are highly empirical and vary based upon the experimental conditions being tested (geometric, evaporative, secondary flows, etc.).

That said, the most commonly suggested correlation for this regime is that provided by Tanasawa and Toyoda [51]. They provide an expression for the SMD of drop sizes generated by a plain-orifice type (nozzle) atomizer into quiescent air under a wide range of conditions. This is given in Equation 2.35.

$$SMD = 47\ \frac{d_o}{u}\left(1 - 3.31\,Oh\right)\left(\frac{\sigma\, g}{\rho_g}\right)^{0.25} \qquad (2.35)$$

2.4.4 Secondary Atomization

In addition to the primary breakup of a liquid jet, researchers mention a process called secondary atomization, whereby the drops produced from the jet further breakup themselves due to internally- and externally-induced instabilities [11, 24]. Meisse provides a treatment and mathematical description of this phenomenon in his paper [29].

Liu [26] provides more current techniques for characterizing this secondary disintegration. However, due to the prohibitively complex nature of this phenomenon, it is not discussed further herein and is considered beyond the scope of the present analysis.

2.5 Jet Heat Transfer

Understanding the exchange of heat between a liquid jet and its environment is important for ensuring safety and efficiency, regardless of the application. As discussed, one of the most important factors needed to determine heat transfer is the area over which this process occurs. Looking at energy equation for a liquid jet in a gaseous environment provided by Kutateladze [23], this becomes readily apparent. Kutateladze's general form of the liquid jet energy equation is given in Equation 2.36.

$$\frac{\partial}{\partial t}\left(\rho_l i_l\right)+\nabla\bullet\left(\rho_l i_l \bar{u}_l\right)=\dot{q}_l'''-\dot{\Gamma}''' i_l+\varepsilon_H\nabla^2\left(\rho_l i_l\right) \quad (2.36)$$

In Equation 2.36, i_l is the liquid enthalpy, $\bar{u}_l$ is the jet velocity vector, $\dot{q}_l'''$ is the heat generation rate in the liquid, $\dot{\Gamma}'''$ is the mass transfer rate, and ε_H is the diffusivity of heat.

Referring to Collier and Thome, the three terms to the right side of Equation 2.39, which respectively describe the energy source from the liquid, energy source from mass transfer (such as condensation or evaporation), and the molecular diffusion of

energy, are directly proportional to the heat transfer area [8]. Collier and Thome suggest a similar equation for a drop, though it does have other considerations. Regardless of the inherent mathematical differences, the surface area remains an important quantity to determine for both the continuous and discontinuous regions of a liquid jet.

One of the first analyses of liquid jet heat transfer is presented by Kutateladze. He studies both laminar and turbulent plane, cylindrical jets. Building this foundation, a number of other researchers [2, 22, 47] develop advancements specifically for laminar jets. This progress is reviewed extensively by DeSalve et al. [10].

Through the course of development, it becomes convenient to describe the empirical correlations developed in terms of the Stanton number. The use of a Stanton number relationship arises from experimental insight into the mechanisms governing heat transfer between jets and their environment [22]. Equation 2.37 provides a mathematical definition of the Stanton number, abbreviated St, often used when describing jet heat transfer.

$$St = \frac{d_o}{4x} \ln\left(\frac{T_g - T_o}{T_g - T_x}\right) \quad (2.37)$$

In Equation 2.37, x is the distance along the jet in the streamwise direction, T_g is the temperature of the gaseous environment, T_o is the jet temperature in the nozzle, and T_x is the jet temperature at distance x.

This thought process is subsequently applied to turbulent jets by Kim and Mills, who account for axial turbulence damps attributed to the surface tension and viscous forces acting on the jet [22]. Celata et al. build upon the research of Kim and Mills, as well as a number of other researchers [18, 22], and derive an expression for the heat transfer coefficient based upon surface instabilities, surface shear, nozzle geometry, and turbulence properties of the jet flow [6].

Though each of these works provides insight into jet heat transfer phenomena, they were also correlated against their own experimental data. Furthermore, the majority of the correlations developed are only valid for a continuous jet, which based upon the previous literature discussed may only exist for a short distance following discharge. In an effort to provide a more robust jet heat transfer model, Takahashi et al. review and compare these correlations, and suggest four of their own, based upon a range of experimental data [50].

Takahashi et al. provide Stanton number correlations for four types of jets. These types are defined by the relative importance of entrainment and interfacial shear on inducing surface disturbances and whether or not break up occurs according to the criteria proposed by Grant and Middleman for turbulent jets. Takahashi et al.'s correlations all follow the general form given in Equation 2.38; however, the coefficients indicated by capital C's change based upon the type of jet being characterized.

$$St = C\, d_o^{\,C} \left(\frac{x}{d_o}\right)^{C} u^{C}\, \nu^{-0.61} \left(\frac{\rho_g}{\sigma}\right)^{0.32} \qquad (2.38)$$

Following breakup, research is also presented studying heat transfer between drops and their environment. This phenomenon is well-documented, and a number of previously discussed references [24, 26] provide a range of correlations and models for specific conditions, nozzle geometries, and applications.

Chapter 3

Mechanistic Characterization of Jet Geometries

There exist a number of liquid jet applications in a variety of disciplines, as previously discussed. With regard to nuclear engineering, the primary application of liquid jets is heat transfer. The mode of heat transfer most often observed with jets in this area is condensation, a process whereby heat is removed from a system by the conversion of vapor to liquid [8].

Heat transfer, in general, requires a sound characterization of the surface area over which energy transport occurs. For condensation, one can appreciate the imperative nature of properly calculating this information, as both mass and heat transfers occur at the interface. Condensation is typically taken to be either a dropwise or filmwise phenomenon, depending upon the conditions and geometries inherent to the physical system [8]. Regardless of the type, describing condensation relies heavily upon the understanding of the interfacial surface. Therefore, an earnest need is apparent for the characterization of liquid jet surface area as applied to the nuclear engineering field.

Literature suggests that a jet is assumed to be either laminar or turbulent [43], exists within any of four primary breakup regimes [35], is broken or unbroken, and has a smooth or disturbed surface [50], depending upon the physical conditions as well as the axial distance traveled from the nozzle [24]. The differences between jets under any combination of these attributes are often quite disparate and are previously discussed; suffice to say that surface area and its physical manifestation varies greatly between them. With such a broad range of conditions described in the literature, it is necessary to determine specifically which regions are of interest.

3.1 Problem Definition

The papers of Celata et al. [6] and Takahashi et al. [50] describe current (at the time of publication) and previous experiments on liquid jet heat transfer. Both publications are explicitly geared toward application in the nuclear engineering realm, which they discuss in detail. As such, the test conditions presented by Celata [6] and Takahashi [50] provide conditions directly related to those in the nuclear engineering-realm. Though these papers involve surface phenomena such as condensation, the present analysis will not; this is beyond the scope of work.

The collective range of liquid jet conditions studied, according to and including these researchers' work, is described in Table 3-1. This collection represents a very diverse set of flow and environmental conditions for liquid jets. In practice, liquid jet conditions cover a

considerably smaller range, as they are dictated by a particular function or use. Table 3-1 also provides a suggested subset of the overall conditions which would be encountered in practice. The bulk of the experimental data accordingly falls within the applicable range.

Table 3-1: Jet conditions reported by Celata [6] and Takahashi [50].

Experimental Range		**Application Range**	
Parameter	**Range**	**Parameter**	**Range**
d_{jet}	0.50 mm - 20.0 mm	Re	10,000 - 250,000
Re	6,000 - 900,000	We	0.20 - 20.0
We	0.15 - 3,000	Oh	$2.0 \times 10^{-6} – 4.0 \times 10^{-4}$
Oh	$4.0 \times 10^{-7} – 1.0 \times 10^{-2}$		

It should be noted that the Reynolds and Weber number ranges listed in Table 3-1 reflect the liquid jet properties, not those of the gaseous environment. Because literature uses both quantities to describe the breakup process, it is important to make this distinction.

As discussed in Chapter 2, the disintegration processes of laminar and turbulent jets are very different. With the introduction of turbulence to an already unstable system, an additional set of considerations is needed to describe the breakup of the continuous stream. This difference is reflected in the disparity between the suggested breakup length expressions for laminar and turbulent jets, given respectively in Equations 2-26 and 2-27. Therefore, it is important to distinguish whether the jets used in nuclear engineering applications are laminar, turbulent, or both.

Using the empirical relation developed by Van de Sande in Equation 2-28 and the range of diameters from Table 2-1, a range of critical Reynolds numbers is found. Knowing that a critical Reynolds number implies a transition from laminar to turbulent flow, the resulting range in Table 2-2 suggests that liquid jets used in nuclear engineering applications will be universally turbulent.

Table 3-2: Range of critical Reynolds numbers for the full range of applicable jet data.

Parameter	Range
d_{jet}	0.50 mm - 20.0 mm
Re_{crit}	1,511 - 2,448

Turbulence is not the only factor in jet disintegration; the mode or regime of breakup is also significant. Table 2-1 provides a numerical description of the transition between breakup regimes. Recalling the Weber number range in Table 3-1 for the applicable data as well as the breakup regime criteria, one finds that most jets will fall within the Rayleigh and FWI breakup regimes.

From this information, a definition of the problem at-hand can be made. The body of work hereafter will characterize the surface area available for heat transfer of turbulent liquid jets in the Rayleigh and First Wind-Induced breakup regimes. Within these regimes, different approaches will be proposed for the continuous and post-breakup or discontinuous jet geometries, as they are dissimilar. Combining the results for each region will allow for the characterization of the entire surface area for a liquid jet of given length.

3.2 Rayleigh Regime

The Rayleigh breakup regime is use to describe the lower Reynolds and Weber number turbulent jets in the range described in Table 3-1. Jet surfaces in this regime exhibit a long, straight section that is undisturbed on a macroscopic scale (on the order of the jet diameter) followed by the brief, but pronounced appearance of wave growth and subsequent breakup. An example of this behavior is provided in Figure 3-1.

Referring to Figure 3-1, one can see that barring the very beginning and end (several jet diameters) of the jet, a smooth surface is observed. As previously discussed, breakup is caused by growth of a 'most dangerous' disturbance, as described originally by Rayleigh and later by a number of other researchers.

Rayleigh postulated [33] that upon breakup, the disturbance leads to the production of one drop, whose volume is equivalent to that of a section of the jet characterized by the disturbance wavelength. Because aerodynamic forces are not a factor in the Rayleigh breakup regime, the surface tends to be relatively smooth and drop production occurs on a uniform basis. This uniform size and spacing is well documented [24, 26] for the Rayleigh regime. Further, this well-defined process, which agrees quite well with theory [54, 56], leads to spherically-shaped drops of relatively uniform size and dispersion. This is also depicted in Figure 3-1.

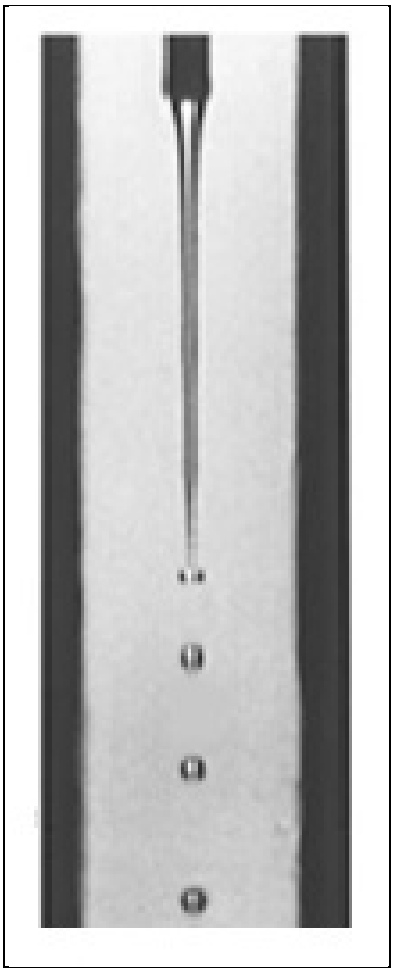

Figure 3-1: Photographic example of a turbulent liquid jet

in the Rayleigh breakup regime [21].

Due to the existence of two primary geometries in the Rayleigh breakup regime, it is logical to suggest that any model of a jet therein should consist of two discrete regions. As such, Figure 3-2 shows a Rayleigh-type jet broken into two axial lengths, l_1 (or l_b) and l_2. These lengths represent the continuous and discontinuous or broken jet lengths respectively. Their sum represents the total jet length being analyzed, L.

Intuitively, the mathematical description of each section or length entails a number of approximation and assumptions unique to the region. The treatment of each region will be described in further detail in the following sections. Additionally, it is assumed that the jet is adiabatic; and as such condensation does not occur. Allowing for mass, momentum, and energy transfer between the jet and its environment would introduce a number of considerations that are beyond the scope of the present analysis.

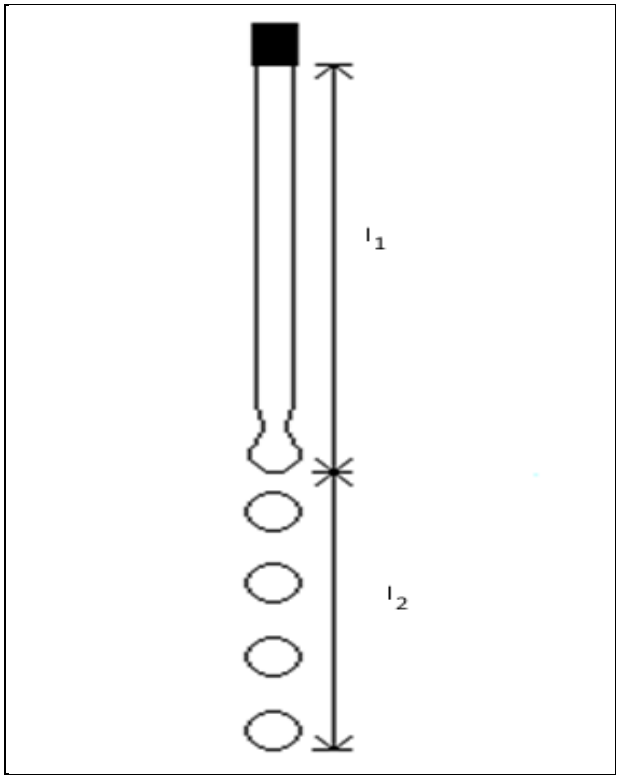

Figure 3-2: Discretization of turbulent liquid jet in the Rayleigh breakup regime.

3.2.1 Continuous Jet Region

The continuous region of the liquid jet, indicated by the axial distance l_1 in Figure 3-2, is relatively straight in the direction of bulk flow and smooth on the surface. This observation is consistent with experiments, as demonstrated in Figure 3-1. Though there is manifestation of the most dangerous disturbance on the jet surface towards end, this typically does not account for any significant axial distance along the jet [21].

It is convenient to describe the surface area in the continuous region in the manner of a right circular cylinder. The expression for the surface area of a right circular cylinder is given in Equation 3.1.

$$A = \pi d_{jet} l_{jet} \quad (3.1)$$

In Equation 3.1 d_{jet} is the jet diameter and l_{jet} is the length of the jet. From this expression, it is apparent that the jet diameter and length are the two quantities needed to calculate the surface area of the continuous region of a Rayleigh-type jet.

The jet diameter is assumed to be constant and equal to nozzle inner diameter. This assumption is consistent with both theory [54] and experiments [21, 35]. Though there can be variations in the diameter due to turbulence, deformation from disturbances, surface tension and inertial forces, they will be assumed to be minor.

The pinching phenomenon prior to breakup/drop formation, also shown in Figures 3-1 and 3-2, is assumed to be negligible when describing the jet diameter. This occurs over a relatively short distance and the change in the jet diameter is relatively small in magnitude [35]. Therefore, a Rayleigh-type jet is assumed to breakup prior to any significant variation or perturbation of the outer diameter, which is assumed constant over the continuous length, l_1.

Similar to the diameter, the continuous length of Rayleigh-type jets has been described by theoreticians [33, 54] and experimentalists [21, 35] alike. However, the best reported agreement between the predicted and measured continuous lengths of liquid jets is attributed to several of the empirically-formulated correlations reviewed in Chapter 2.

Literature suggests use of the expression given by Grant and Middleman [13]for turbulent jets given in Equation 2.25 [24, 26]. Though this is an older correlation of data, it has been proven to be robust in its applicability and relatively successful in characterizing the continuous length of Rayleigh-type jets [11]. However, the more recent data collected and compiled first by Sallam et al.[39] and later Sallam and Faeth [38], combined with that of previous researchers suggested a new, more agreeable correlation could be made more specific for turbulent, Rayleigh-type jets.

Figure 2-12 shows this data concurrent with the correlations developed by Grant and Middleman [13] and Sallam et al [39]. Sallam et al.[39] reported that their agreement with data in the Rayleigh regime was found to be better than that of Grant and Middleman and within the experimental uncertainties associated with the data of other researchers [39]. The usage of the correlation of Sallam et al. [39] requires assuming a number of things about the continuous region of a Rayleigh jet.

First, the assumption of a constant diameter is again invoked, as the Weber number is proportional to this quantity. Second, it is assumed that the bulk fluid properties can used to describe the jet. Further, these properties are assumed to be constant over the continuous length. Any variation in these properties would result in a varying Weber number. Third, the velocity of the jet is also described using a bulk value. In reality, there will be some velocity profile existent in the jet flow which will change over the axial length. However, this phenomenon is assumed to be captured within the correlation.

Knowing that the continuous jet diameter is assumed to be constant and that the breakup length can be expressed using the correlation of Sallam et al [39], Equation 3.1 can be rewritten as Equation 3.2.

$$A = 5.0 \pi d_o^{\,2} We^{0.5} \quad (3.2)$$

3.2.2 Discontinuous Jet Region

It has been shown that at some length, l_1, Rayleigh-type turbulent jets will breakup to form round drops. These drops have a different, yet related geometry compared to the continuous region of the jet. Calculating the surface area of the discontinuous region of a Rayleigh jet thus requires a different set of considerations. Where the continuous region required knowledge of the diameter and length, the discontinuous region can be described knowing the number, size, and spacing of drops, as this information will describe the drop surface area following the continuous region occupied by liquid. This is described in Equation 3.4.

$$A = n_d \, \overline{A}_d \quad (3.3)$$

In Equation 3.3, n_d is the number of drops and A_d is the mean drop surface area of one drop in the discontinuous region.

As previously discussed, drops produced in the Rayleigh regime are typically uniform in size and shape [26, 35]. Drops also tend to be spherical in shape, as opposed to elliptical [38]. Common literature suggests that theoretical analysis can provide reasonable insight into drop size and the work of Tyler is directly suggested by a number of sources [35, 56].

Tyler's approach holds due to the uniformity observed within and theoretically inherent to the Rayleigh breakup regime. Liquid jet breakup and drop formation are directly related to a dominant disturbance whose wavelength and magnitude are proportional to the issuing nozzle inner diameter. Therefore, it is logical that the drop size will also scale proportionally with nozzle diameter, as aerodynamic effects are negligibly existent in the Rayleigh breakup regime [35]. This assertion is also based upon the assumption that a jet will produce one drop upon breakup in the Rayleigh regime [35, 54]. Because this assumption has been confirmed experimentally and commonly adopted in analyses, it will be used in the present analysis.

Through the years, researchers have found that there is some minor deviation the proportionality constant suggested by Tyler [54]. Teng presents an analysis of drop size in for turbulent jets with Ohnesorge numbers characteristic of the Rayleigh breakup regime [52]. Recalling the analysis of Teng [52], surface deformation in the continuous region is assumed to be controlled by the fastest growing disturbance, where each wavelength of its magnitude produces a single, spherical drop upon breakup. Teng [52] relates the mean size of drops produced to a modified Ohnesorge number.

The concept of uniformity in the Rayleigh regime is reinforced; however, as the variation of Oh number (found using Tables 2-1 and 3-1) is nearly two orders of magnitude and the expression developed by Teng et al. [52] shows a variation in the predicted mean drop diameter of approximately two thousandths. This is given in Table 3-3.

Consequently, Teng et al. [52] suggest a value of 1.88 as a constant of proportionality applied to Rayleigh's breakup theory for this region. Because the results of Teng et al. [52] agree more closely with experimental data that that of Tyler [54], a commonly accepted approached for this region, the present analysis will use the expression given by Teng et al. [52] to describe drop diameters in the discontinuous region of the Rayleigh regime.

Table 3-3: Variation of predicted drop diameters within the full range of applicable data.

Oh	**d/d_o - Tyler**	**d/d_o - Teng**
$2.0x10^{-6}$	1.91	1.8827
$4.0x10^{-4}$	1.91	1.8818

The number of drops is also required to describe the surface area in the discontinuous Rayleigh region. Kerst [21] and Sallam et al. [39] suggest that this spacing is uniform immediately following jet disintegration or breakup and is on the order of the diameter of drops produced, assuming a spherical shape. However, it is intuitive to suggest and further experimental photographs confirm that this spacing changes as drops descend from the point of breakup. These variations can be attributed to aerodynamic drag and gravitational acceleration.

Regardless of the source for spacing change, it is necessary to define some means of calculating the number of drops that does not require spatial information. Invoking the continuity between the continuous and discontinuous regions and assuming no sources or

sinks of mass (or flow) are present, the conservation of mass between geometries can be written as Equation 3.4.

$$(\rho u A)_{jet} = n_d (\rho u \overline{A})_d \quad (3.4)$$

Assuming that the variation of the liquid density between the continuous and discontinuous geometries is negligible, Equation 3.4 can be rewritten in terms of the number of drops in the discontinuous region. This expression is given in Equation 3.5.

$$n_d = \frac{(u A)_{jet}}{(u \overline{A})_d} \quad (3.5)$$

Recalling Equation 3.3, the number of drops given by Equation 3.5 can be substituted to obtain a new expression for the surface area in the discontinuous region. This is given as Equation 3.6.

$$\overline{A} = \frac{(u A)_{jet}}{u_d} \quad (3.6)$$

Though the quantities in Equation 3.6 can be determined experimentally, it is customary to describe relations in terms of dimensionless numbers. As such, a number of fluid properties such as the density, surface tension, and viscosity can be multiplied by the numerator and denominator of this expression. Again assuming negligible property variation

between geometries, the area of the discontinuous region of a turbulent, Rayleigh-type jet can be written in terms of the Reynolds and Weber numbers as shown in Equation 3.7.

$$\overline{A} = \pi d_o^{\,2}\left(\frac{We}{We_d}\right)\left(\frac{Re_d}{Re}\right) = \pi d_o^{\,2}\left(\frac{Oh}{Oh_d}\right)\left(\frac{We}{We_d}\right) \quad (3.7)$$

This expression is important for a number of reasons. First, no direct assumptions are required for drop sizing or spacing. The previously-discussed correlation provided by Teng et al [52] is suggested to evaluate data if drop diameter measurements are not taken under desired conditions; however, this is not immediately required in the present analysis.

Second, the area is expressed in terms of known or commonly-measured quantities, the nozzle diameter and Reynolds and Weber numbers. As these numbers are typically used to describe ranges or sets of data, the present analysis finds it appropriate to provide an expression related to them. This form suggests an ease of both implementation and usage.

3.3 First Wind-Induced Regime

Similar to Rayleigh-type jets, jets in the First Wind-Induced or FWI regime can exhibit a number of different geometric configurations throughout their axial length. Also like Rayleigh jets, this behavior suggests that liquid jets in the FWI regime should be discretized to account for geometric disparities when calculating the surface area. Unfortunately, the FWI breakup regime is far less described and/or understood, as indicated

by available literature [24, 26]. Further, the importance of aerodynamic forces in the FWI regime also proves to complicate its overall description.

Figure 3-3 is a high speed photograph, again taken by Kerst in a series of experiments regarding the breakup of liquid jets [21]. The conditions present in the photograph place this jet somewhere in the mid-We values of the FWI breakup regime.

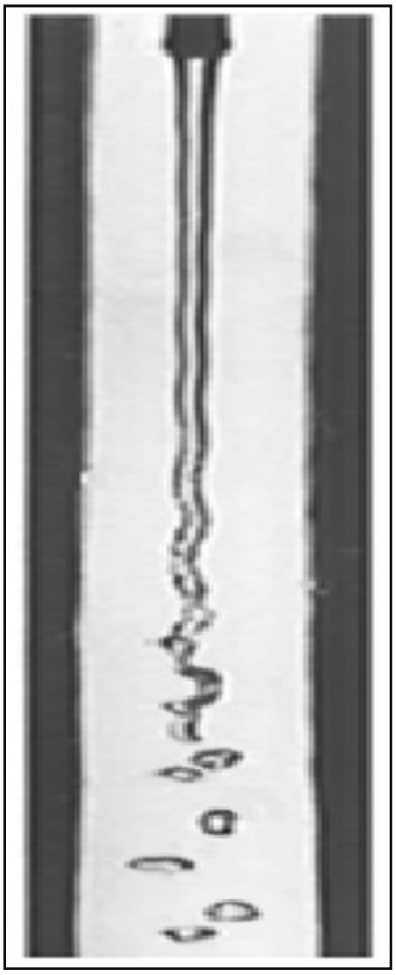

Figure 3-3: Photographic example of a turbulent liquid jet in the FWI breakup regime [21].

The disturbance effects of aerodynamic forces on the surface of the jet are immediately apparent from Figure 3-3. In contrast to the Rayleigh regime, there is a large amount of surface distortion or perturbation prior to breakup. As stated in Chapter 2, these distortions are the result of turbulence in the bulk flow, surface tension, and aerodynamic interaction between the surface of the jet and its environment. All of these quantities are far more pronounced in the FWI regime compared to the Rayleigh regime, due to the higher Weber and (typically) Reynolds numbers [21].

It is important to note, however, that surface tension remains the dominant cause of jet breakup in this region [24, 35]. Thus, the effects of turbulence act to enhance the preexisting disturbances and their growth rates, while those aerodynamic interaction act as a damping force until sizable perturbations are formed.

With the surface instability caused by the surface tension being more pronounced and the enhancement to the growth of this instability via turbulent momentum and energy exchange, a new geometry can be observed in the FWI regime. Following a straight, elongated region of continuous jet, similar to that found with Rayleigh jets, the bulk flow of the jet is sometimes observed to deform in an oscillatory or wavy manner. This is dependent upon the flow and environmental conditions, and is observed in Figure 3-3.

As the Weber and/or Reynolds numbers of jets are further increased within the FWI regime, the waves created in the bulk flow of the jet can form ligaments [57]. These ligaments act much like the continuous waves of the jet, as they have a bulk flow in the

streamwise direction, oscillate, and break up to produce one or more drops [57, 58]. Sallam et al [39] studied this phenomenon and were successfully able to predict the onset of what the present analysis considers surface disturbances (prominent waves and subsequent ligament formation) [39]. The data and correlations proposed by Sallam et al. [39] are depicted in Figure 3-4.

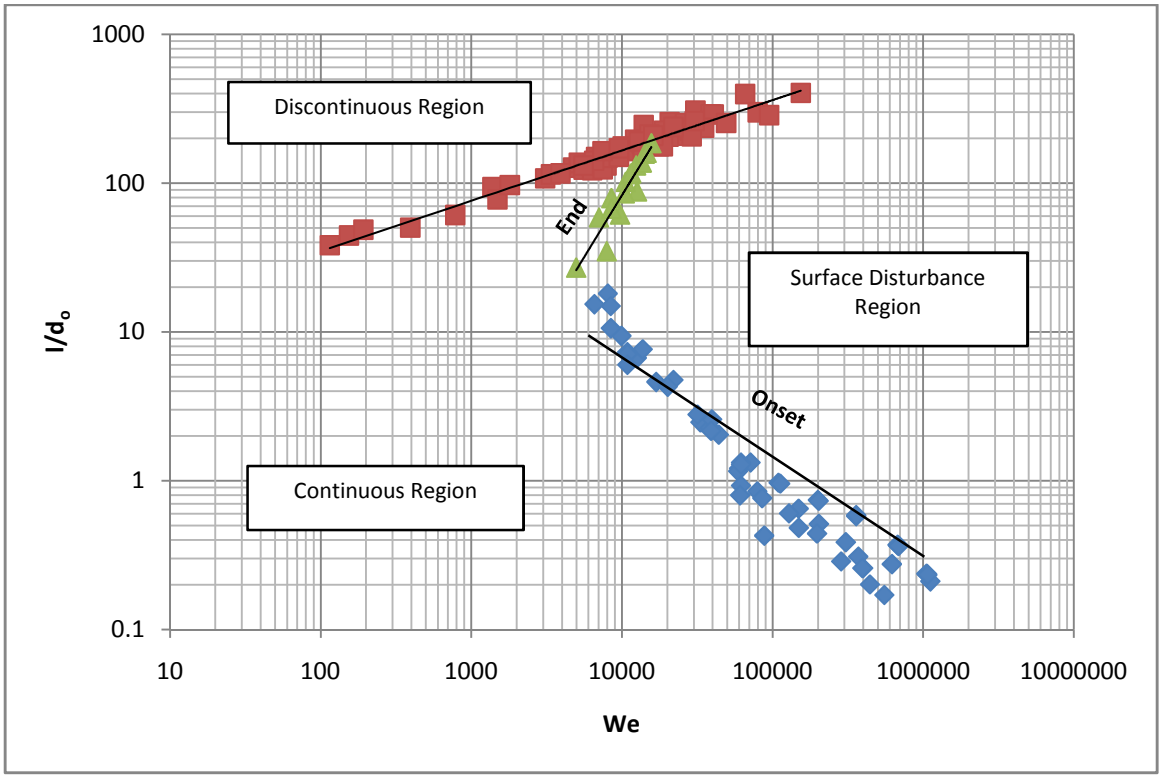

Figure 3-4: Disintegration data and characteristic lengths for turbulent liquid jets in the Rayleigh and FWI breakup regimes [39].

One can see that there is good agreement with experimental data in all cases except for the onset of surface disturbances. Refitting this line, much better agreement with the data is found, and is pictured in Figure 3-5 which highlights the FWI regime conditions.

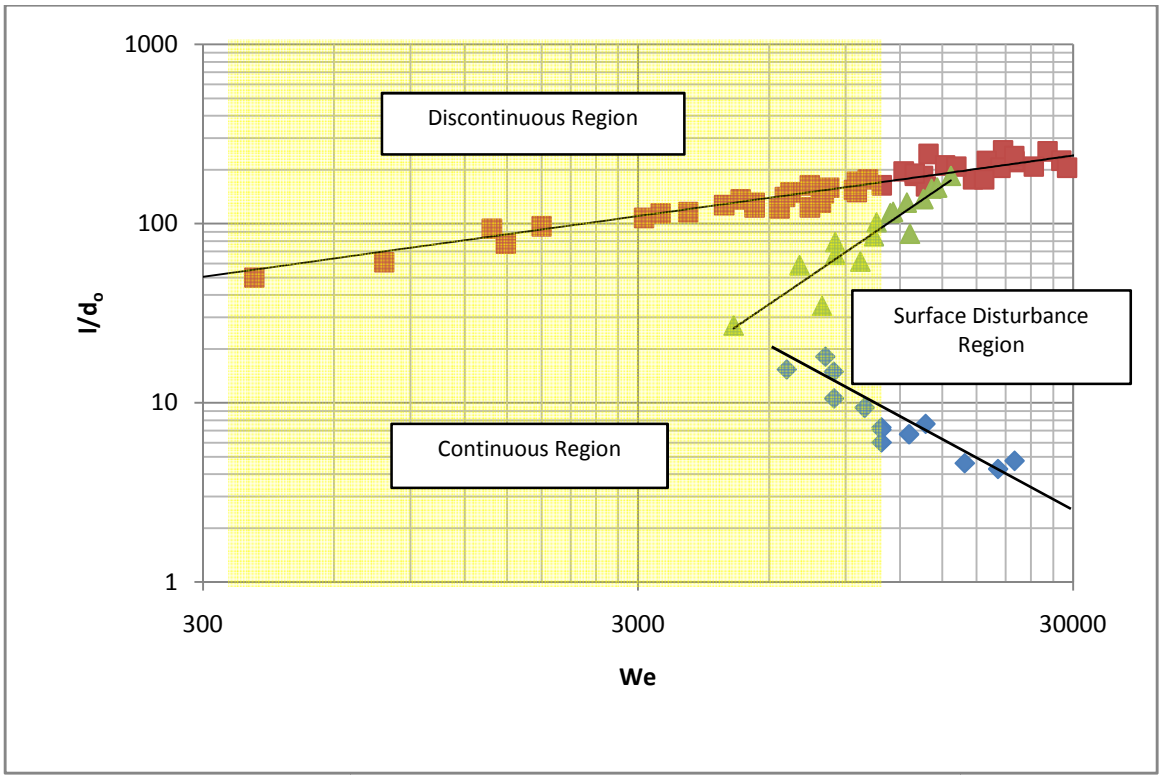

Figure 3-5: Disintegration data and characteristic lengths for turbulent liquid jets in the FWI breakup regime according to Sallam et al. [39] and the present analysis.

The expression for the line describing the onset of surface disturbances is given in Equation 3.7. In this expression l_o indicates the streamwise distance from the nozzle at which the jet surface becomes visibly perturbed and enters the surface disturbance region.

$$l_o = 1.87x10^4 \, We^{-0.851} \quad (3.7)$$

Figure 3-5 shows that jets in the FWI regime (the highlighted region) can either act like those in the Rayleigh regime and possess continuous and discontinuous geometries, or they can develop surface disturbances prior to breakup and have three discrete geometries: continuous, disturbed, and discontinuous. Sallam et al. delineate this transition with a Weber number of approximately 5,000 obtaining satisfactory agreement with experimental data [39].

Also visible from Figure 3-5 is the fact that FWI jets can transition out of the surface disturbance region prior to breakup. It appears that jets characterized by Weber numbers between 5,000 and 16,000 would revert to a straight, continuous geometry; however, this is not the case. One can observe this transition in Figure 3-3, whereby the disturbed surface begins to form ligaments, as previously discussed.

When the line indicating this transition intersects that of jet breakup it is assumed that ligament formation will occur throughout the surface disturbance region. This occurs for Weber numbers greater than 16,000, as shown in Figure 3-5. Surface disturbances become extremely pronounced due to aerodynamic resistance and ligaments are subsequently formed intermittent with surface disturbances. However, such a behavior is more characteristic of the SWI regime than the FWI regime.

Therefore, if jets are beyond the Weber number transitions proposed by Sallam et al [39], they can be considered to transition between continuous, disturbed, ligament, and discontinuous states. It is also of note that the ligaments formed in the FWI regime are

predominantly similar in size and shape to their parent disturbances [39, 57]. In other words, it is logical to approximate the surface area of the ligaments in the same manner as the surface disturbances preceding them. Experimental data [39, 57] suggests that this approximation should be reasonably valid for the FWI regime. However, due to the more erratic nature of the SWI regime, it cannot be extended further.

Based upon these observations, the present analysis will divide jets in the FWI regime into either two or three regions, based upon the Weber number criteria given by Sallam et al [39]. If the jet Weber number is less than or equal to 5,000, then it will be comprised of two regions, continuous and discontinuous. This is analogous to the Rayleigh jet discretization shown in Figure 3-2. Conversely, if the jet Weber number is above 5,000, it will be comprised of three regions, continuous, surface disturbance, and discontinuous. This discretization is shown in Figure 3-6.

Figure 3-6 suggests that a turbulent liquid jet in the FWI breakup regime be discretized into three axial lengths, l_1, l_2, and l_3. These lengths represent the continuous, surface disturbance, and discontinuous or broken jet lengths respectively. Their sum represents the total jet length being analyzed, L. The mathematical treatment of each region is described in the following sections.

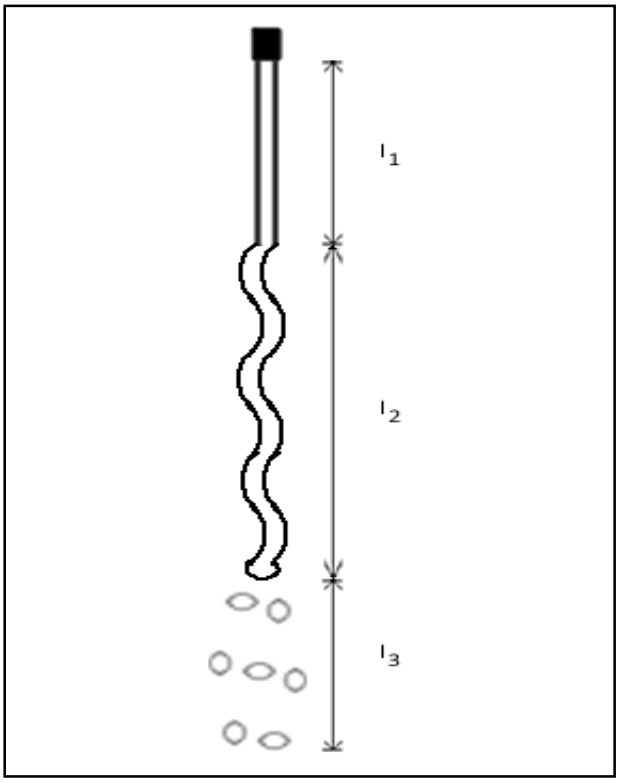

Figure 3-6: Discretization of turbulent liquid jet in the FWI breakup regime.

3.3.1 Continuous Jet Region

Similar to that of the Rayleigh regime, the continuous region of a turbulent liquid jet in the FWI regime, indicated by the axial distance l_1 in Figure 3-6, is relatively straight in the direction of bulk flow and smooth on the surface. This observation is consistent with experiments, as demonstrated in Figure 3-3. Though there is disturbance growth occurring throughout this jet length, it is assumed to have minimal affect on the jet surface. However, once this disturbance becomes pronounced, a transition take place either to the surface

disturbance region or the discontinuous region based on the Weber number characterizing the jet, indicated respectively in Figures 3-6 and 3-3.

It is convenient to describe the surface area in the continuous region in the manner of a right circular cylinder, as given Equation 3.1. Also similar to the Rayleigh regime, the jet diameter and length are the two quantities needed to calculate the surface area for this region of a FWI-type jet.

The jet diameter is assumed to be constant and equal to nozzle inner diameter. This assumption is consistent with experimental observations [21, 38]. Though there can be variations in the diameter due to aerodynamic forces, turbulence, deformation from disturbances, surface tension and inertial forces, they will be assumed to be minor specifically in this region.

In addition to the diameter, a number of researchers have proposed correlations for the continuous length of FWI-type jets [13, 24, 39]. Much like for Rayleigh jets, texts suggests use of the expression given by Grant and Middleman [13] for turbulent jets. However, the more recent data collected and compiled by Sallam et al. [39], combined with that of previous researchers suggests a new, more agreeable correlation could be made more specifically for turbulent jets in FWI regime.

As Figure 3-5 shows, the expression reported by Sallam et al. [39] was found to be in much closer agreement with available data than that of Grant and Middleman [13]. For this reason, the continuous length of turbulent, FWI-type jets will be calculated using the correlation of Sallam et al. As this correlation is related to the jet Weber number, its usage requires assuming a number of things about the continuous region of a FWI jet.

First, the assumption of a constant diameter is again invoked, as the Weber number is proportional to this quantity. Second, it is assumed that the bulk fluid properties can used to describe the jet. Further, these properties are assumed to be constant over the continuous length. Any variation in these properties would result in a varying Weber number. Third, the velocity of the jet is also described using a bulk value. In reality, there will be some velocity profile existent in the jet flow which will change over the axial length. However, this phenomenon is assumed to be captured within the correlation.

Knowing that the continuous jet diameter is assumed to be constant and that the breakup length can be expressed using the correlation of Sallam et al [39], Equation 3.1 can be rewritten as Equation 3.8 to describe the surface area of the continuous region of a turbulent FWI-type jet with a Weber number less than or equal to 5,000.

$$A = 2.1\pi d_o^{\,2} We^{0.5} \qquad (3.8)$$

If the jet Weber number is greater than 5,000, Equation 3.8 must be rewritten to account for the axial length along the jet in the surface disturbance region prior to breakup. Using the correlation provided by the present analysis in Equation 3.7, the surface area of the continuous region of a turbulent FWI-type jet with a Weber number above 5,000 is written as Equation 3.9.

$$A = \pi d_o \left(l_b - l_o \right) \quad (3.9)$$

In Equation 3.9, l_b is the breakup or continuous length of the jet determined using Equation 2.27 and l_o is the length for the onset of surface disturbances determined using Equation 3.7.

3.3.2 Surface Disturbance Region

When jets in the FWI breakup regime exceed a Weber number of approximately 5,000, researchers [21, 39] have observed the formation of pronounced disturbances on their surfaces. These disturbances are similar to those causing breakup in the Rayleigh regime, but are accentuated primarily by increased turbulence and aerodynamic resistance in the FWI regime.

This occurs to such a dramatic extent that the bulk jet flow is distorted in the cross-flow direction in the shape of waves or oscillations. Such behavior is exhibited in Figure 3-4. As the straight jet is deformed, the diameter is also reduced to conserve mass, assuming the absence of any external source. Thus, in order to calculate the surface area of turbulent FWI jets in this region, the number, size, and shape of these disturbances must be quantified.

Assuming the applicability of the transition line proposed by Sallam [39] and refitted in the present analysis, the average number of oscillations or waves can be determined by combining the axial length of the surface disturbance region with the size and shape information for the waves. In this manner, one can solve for the number of waves, n_w, as given in Equation 3.10.

$$\bar{n}_w \cong \frac{l_2}{z} = \frac{l_b - l_o}{z} \quad (3.10)$$

In Equation 3.10, l_2 is the length of the surface disturbance region and z is length of a single disturbance in the streamwise direction. This formulation assumes that all waves are uniform in size and that there are only two distinct jet geometries prior to breakup.

The observations of Sallam et al. [39] and Wu and Faeth [57] suggest that assuming a uniform wave or disturbance size in this region for FWI jets is a reasonable approximation. Though growth does occur as waves propagate along the jet in the streamwise direction, their variation in size is predominantly less than an order of magnitude.

Regardless of size uniformity, however, the physical geometry of the disturbances must be quantified to determine the surface area of the jet in this region. Since the source of the disturbances is related to both the turbulence present in the bulk jet flow and the instability caused by aerodynamic resistance on the jet surface, it is logical to suggest that disturbance magnitude or size is also a function of these forces. This assumption is consistent with the work of Sallam et al. [39] and Wu and Faeth [57], who suggest that proportionality exists between the turbulent eddy size and surface disturbance size and shape.

Sallam et al. and Wu and Faeth propose an analysis whereby small droplets of liquid are sheared off of the crests of these disturbances, thus invoking the constructs of a classical Kelvin-Helmholtz instability. However, they also relate the size of the droplets formed to the size of turbulent eddies present in the bulk jet flow. Because the size of the droplets is directly related to the surface disturbance leading to their formation, characterizing the turbulent eddies provides insight into the sizing of surface disturbances.

It should be noted that Sallam et al. [39] and Wu and Faeth [57] are primarily concerned with jets whose physical conditions lie within the SWI regime, as this is where secondary droplet production is most prevalent. The present analysis aims to extend this theory into the FWI regime, as the same surface disturbances are present; they are simply lesser in magnitude and result predominantly in jet breakup prior to secondary droplet production [21].

Assuming an elliptically-shaped disturbance, Figure 3-7 illustrates the relation between the size and shape of turbulent eddies and surface waves. In Figure 3-7, *y* is the cross-stream disturbance length, *z* is streamwise disturbance length, and the eddy size is related to the cross-stream auto-correlation distance, Λ.

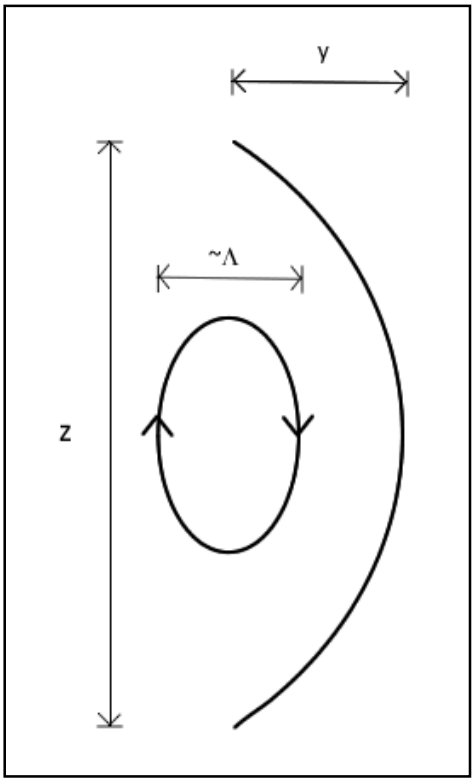

Figure 3-7: Depiction of a turbulent eddy and surface disturbance for a turbulent liquid jet in the FWI breakup regime.

An elliptical shape is assumed for the disturbance based upon both experimental observations and turbulent pipe flow theory. Sallam et al. and Wu and Faeth suggest that the turbulence present in a free-stream jet flow is analogous to that of a pipe flow, as described by Hinze [16]. They also suggest that the turbulence present in the jet flow is a direct

consequence of that generated prior to and within the issuing nozzle. A number of other researchers have proposed similar theories and have found satisfactory results when comparing to data.

Classically, the largest eddies present in turbulent pipe flows are taken to be on the order of the autocorrelation distance, Λ [16, 58]. The autocorrelation distance is a spatial scale that provides a measure of the longest connection (or correlation distance) between two points in a turbulent flow separated by either distance or time. This distance is used as it is relatively easy to determine experimentally, as opposed to a number of other parameters utilized in turbulence theory. In this case, the separation between two points is assumed to be the cross-stream distance at a given time. Therefore, according to the aforementioned relation proposed by Hinze [16], the cross-stream size of the turbulent eddies present is assumed to be on the order of the cross-stream autocorrelation distance.

In both turbulent pipe flow and wavy jet flow in the surface disturbance region a number of researchers have noted the elliptical geometry of eddies and waves [16, 39, 57]. This behavior is illustrated in Figure 3-8, which demonstrates the relation between the two. Since the streamwise dimension of these bodies cannot be assumed equal to that of the cross-stream direction, a constant of proportionality must defined. Wu and Faeth [57] refer to this consideration as the ellipsicity, or ε. The present analysis will adopt the definition of this parameter given by Wu and Faeth [57], which is the ratio between the streamwise and cross-stream diameters of a drop.

In their experiments, Wu and Faeth [57] were able to measure the volume-averaged ellipsicity of droplets as a function of the normalized distance from the nozzle. Their results are plotted in Figure 3-8. Wu et al. [58] reported and the present analysis confirms that fitting a line to this data, regardless of the type, is met with marginal results at best. The closest agreement is reflected by a correlation coefficient value of less than 0.58 for a power-fit curve.

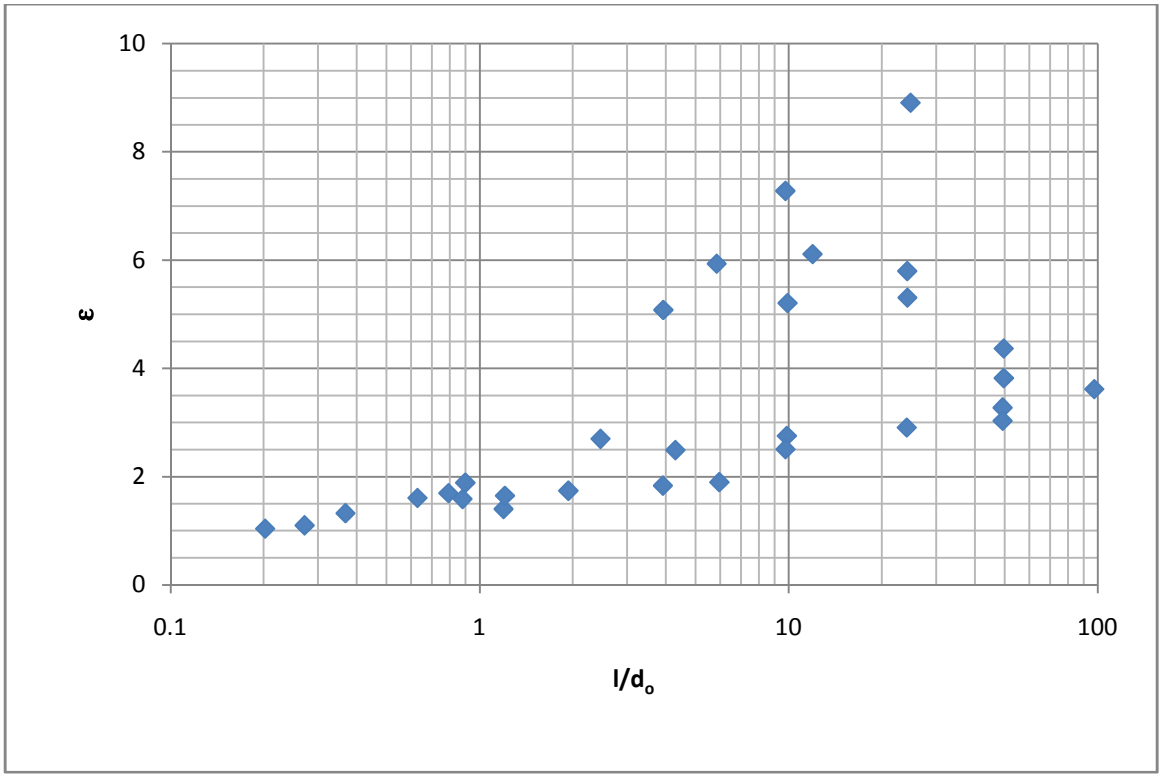

Figure 3-8: Ellipsicity of droplets based upon the normalized streamwise distance from the nozzle for turbulent jets in the wind-induced regimes [57].

Based upon the data shown in Figure 3-8 and the observations made by Wu and Faeth [57] regarding an inability to correlate it, the present analysis suggests determining the range of interest for the normalized axial distance associated with the surface disturbance region and obtaining the ellipsicity by one of two means. Either the data could be averaged over this range to provide a reasonable estimate of the ellipsicity or specific ellipsicity data could be measured over the same range for a given set of conditions.

Assuming that the ellipsicity is known, the cross-stream and streamwise dimensions of the surface disturbances can be written as Equations 3.11 and 3.12, respectively.

$$y \cong \Lambda \quad (3.11)$$

$$z = \varepsilon\, y \quad (3.12)$$

Recalling the assumption of an elliptical shape for the disturbances, Equations 3.11 and 3.12 can be used to calculate half of the perimeter of an ellipse. The resulting expression for p, the arc length of a surface disturbance is given in Equation 3.13.

$$p = \frac{\pi}{2\sqrt{2}}\, y\left(\varepsilon^2 + 4\right)^{0.5} \quad (3.13)$$

This equation is written for an average value of ε; however this can be expressed in terms of an empirically derived expression from future experimental results.

It can be inferred from the analyses and photographs of Kerst [21] that the jet diameter in this region can also be expressed in terms the cross-stream disturbance dimension, or the largest turbulence scales present in the jet flow [39]. This appears to be a reasonable assumption, as both Sallam et al. [39] and Wu and Faeth [57] suggest that the reduced jet diameter in the surface disturbance region is a function of turbulence scales present in the jet flow.

Both use a value of Λ equal to 1/8 of the nozzle inner diameter, consistent with that suggested by Hinze [16] for turbulent pipe flow [16]. Their results, which calculate mean droplet sizes produced in secondary droplet formation in the SWI regime, agree reasonably well with experimental data. Therefore, the present analysis will adopt assume this expression for Λ, the cross-stream correlation distance.

However, as ligament size and shape can vary greatly within the disturbance region, it becomes necessary to assume that an average diameter is adequate to describe these geometries. This dimension would be very difficult to ascertain through experiments, so continuity can be invoked to provide an expression in terms of more measureable quantities. A conservation of mass yields the expression given in Equation 3.14 for the average ligament diameter, d_l.

$$d_l^{\,2} = d_j^{\,2} \frac{u_j}{u_l} \quad (3.14)$$

With this information, an expression for the area of the surface disturbance region can be written in the form of Equation 3.15.

$$A = \pi d_l n_w p \quad (3.15)$$

The equations for the average ligament diameter, number of disturbances, and the perimeter of one disturbance can be substituted into Equation 3.15. Following the same approach used in the Rayleigh discontinuous region, an expression for surface area in the FWI surface disturbance region of a turbulent jet can be written as Equation 3.16.

$$A = \frac{\pi^2}{2\sqrt{2}} d_o \left(\frac{We}{We_{lig}} \right) \left(\frac{\mathrm{Re}_{lig}}{\mathrm{Re}} \right) \left(1 + \frac{4}{\varepsilon^2} \right)^{0.5} = \frac{\pi^2}{2\sqrt{2}} d_o \left(\frac{Oh}{Oh_{lig}} \right) \left(\frac{We}{We_{lig}} \right) \left(1 + \frac{4}{\varepsilon^2} \right)^{0.5} \quad (3.16)$$

3.3.3 Discontinuous Jet Region

Albeit a jet or spray, a large amount of research has been conducted attempting to develop an expression for drop diameters in high Weber number flows. For a jet, this work focuses on the region after breakup, or what the present analysis calls the discontinuous region. Because such work, mainly in the field of combustion, is focused upon drop production as opposed to the solid geometry, the conditions studied tend to fall in the FWI, SWI, and pure atomization breakup regimes for liquid jets.

Similar to their Rayleigh-type counterparts, FWI-type jets produce a number of drops upon breakup. However, because the breakup process of FWI jets is relatively more complex, it follows that the characterization of these drops is also more complex. Variations in size and shape prohibit the use of a theoretical or classical analysis on any practical level [26]. Therefore, the ability of the present analysis to characterize the surface area of the discontinuous region of FWI jets will rely solely upon empirical correlations.

As the geometry is that of discrete, dispersed drops of liquid, an expression for the surface area can be written as Equation 3.17.

$$A = n_d \, \overline{A}_{d,smd} \quad (3.17)$$

In Equation 3.17, n_d is the number of drops and $A_{d,smd}$ is the mean area of one drop based upon the Sauter mean diameter.

Chapter 2 discusses the correlations developed by several researchers that are universally accepted in jet disintegration literature. Though the correlation developed by Tanasawa and Toyoda [51] is quite robust in its range of applicability, it tends to over-predict drop sizes for conditions representative of the FWI regime, while it provides reasonably good agreement in the SWI and pure atomization regimes. Harmon's fit of Meisse's water data [15] also tends to over-predict drop sizes, only to a much greater magnitude than Tanasawa and Toyoda [51]. This can most likely be attributed to the relative age and narrow conditions inherent to Meisse's data [29].

That said, more recent literature [11, 26] tends to reference the correlation developed by Wu et al. [58], given in Equation 2.34. This expression is reported to agree almost universally well within an order of magnitude with drop size distributions found experimentally for conditions representative of the FWI regime. Further, drop ellipsicity, which is observably present in the FWI regime and shown in Figure 3-9, was not reported to have a prohibitively large effect on these predictions – as Wu et al. [58] assume perfectly spherical drops.

Therefore, as the correlation of Wu et al. [58] provides the closest agreement with data for turbulent jets in the FWI regime, the present analysis will implement it as a means of characterizing the mean drop size in the discontinuous region.

As previously discussed, the discontinuous region of turbulent FWI jets is much less uniform than that of Rayleigh jets. However, the same methods can be used to describe the number of drops present in the discontinuous region of a turbulent FWI jet. Invoking continuity between the continuous and discontinuous phases, one finds that the number of drops in the FWI discontinuous region can be expressed as given in Equation 3.18.

$$n_d = \left(\frac{A_{jet}}{\overline{A}_{smd}} \right) \left(\frac{u}{u_d} \right) \quad (3.18)$$

Substituting Equation 3.18 into 3.17, and multiplying by a number of fluid properties such as the density, surface tension, and viscosity, and again assuming negligible property variation between geometries, the area of the discontinuous region of a turbulent, FWI-type jet can be written in terms of the Reynolds and Weber numbers as shown in Equation 3.19.

$$\overline{A} = \pi\, d_o^{\,2} \left(\frac{Oh}{Oh_{smd}} \right) \left(\frac{We}{We_{smd}} \right) \quad (3.19)$$

Chapter 4

Conclusions and Recommendations for Future Work

The study of liquid jet disintegration is important to a number of applications, including the nuclear engineering field. As many of these applications involve the transfer of heat under adverse conditions, a sound understanding is imperative to ensuring safety, efficiency, and predictability. Being able to understand this phenomenon entails describing the mechanisms governing the formation and disintegration of jets, as well as characterizing the specific geometries encountered by jets under a variety of conditions.

The formation and disintegration of liquid jets has been studied for over 150 years by researchers in an array of technical fields. Physicists, mathematicians, and engineers have all found some utility in describing this process; albeit in a qualitative or quantitative manner. Throughout this time, models and correlations have evolved from numerical fits of a narrow band of experimental data to the hybrid correlations utilized by the present analysis which posses both theoretical and empirical bases.

Beyond the mechanistic view of jet formation and disintegration, researchers have also identified a number of different geometries exhibited by jets. The specific geometries observed are direct result of the initial jet diameter, velocity, and fluid properties, the fluid

properties of the gaseous environment surrounding the jet, and the distance traveled from the nozzle exit. Similar to the treatment of the jet disintegration phenomenon, researchers have proposed a number of correlations involving both theoretical and empirical concepts to describe the different sizes, shapes, and distortions of a jet in continuous and discontinuous forms.

Chapter 2 provides an extensive review of the literature available regarding the characterization of liquid jets. Throughout the description, it is apparent that a large amount of work has been competed in a number of very specific areas pertaining to the overall subject of jet disintegration. However, there are very few instances where this range of information is combined to provide a more robust view of this subject.

Therefore, the goal of the present analysis is to develop an approach for the holistic characterization of liquid jet disintegration. In other words, from the moment of exit until some length of interest, a method is to be developed whereby the physical behavior and appearance of jet would be adequately described. As most liquid jet applications in nuclear engineering involve condensation heat transfer, the adequacy of this description is established in the ability to characterize the surface area of a jet under prototypical conditions.

Based upon the observations and recommendations of previous work, it is determined that the scope of the present analysis entailed characterizing the surface area for turbulent, liquid jets in the Rayleigh and first wind-induced breakup regimes. Chapter 3 provides the

detailed analysis and resulting expressions for the surface area of jets throughout the entirety of these regimes. Table 4 provides a summary of the proposed expressions.

Table 4-1: Surface area expressions for various jets conditions.

Axial Region	**Rayleigh Jet**	**FWI Jet**
Continuous	$5.0\pi d_o^{\,2} We^{0.5}$	$2.1\pi d_o^{\,2} We^{0.5}$ OR $\pi d_o \left(l_b - l_o\right)$
Surface Disturbance	n/a	$\frac{\pi^2}{2\sqrt{2}} d_o \left(\frac{Oh}{Oh_{lig}}\right)\left(\frac{We}{We_{lig}}\right)\left(1+\frac{4}{\varepsilon^2}\right)^{0.5}$
Discontinuous	$\pi d_o^{\,2}\left(\frac{Oh}{Oh_d}\right)\left(\frac{We}{We_d}\right)$	$\pi d_o^{\,2}\left(\frac{Oh}{Oh_{smd}}\right)\left(\frac{We}{We_{smd}}\right)$

The intended use of the surface area expressions provided is the advancement of the current state of calculating liquid jet condensation heat transfer, as is of importance in the nuclear engineering field. Available correlations rely upon a number of approximations that are inconsistent with experimental observations to quantify the heat transfer without directly determining the interfacial area. Further, most of these correlations are only valid for a continuous jet geometry, which leaves a substantial portion of the heat transfer underestimated or unaccounted for.

Intuitively speaking, implementing the surface area expressions given in Chapter 3 over the various regions should allow for a more accurate representation of the heat transfer taking place between a jet and its gaseous environment. However, it was also discussed in Chapter 3 that some testing must be undertaken to validate and implement these expressions. Though the present analysis employs and builds upon number of well-regarded previous studies, it is essential to obtain prototypical experimental data.

Chapter 3 also discusses two possible areas of research that could be better characterized to improve the accuracy of the surface area predictions, eddy/droplet ellipsicity, ε, and the autocorrelation distance, Λ. Both of these quantities are estimated in the present analysis, and as such represent a possible source of error. Therefore, it is recommended that testing be undertaken to quantify these values for a more specific set of jet conditions.

Possible testing methods are described in detail by the researchers who proposed values for the ellipsicity and autocorrelation distance. Chapter 3 references this literature, which due to its complexity will not be discussed further.

A final suggestion for future work would be the inclusion of secondary disintegration in the formulation of the surface area in the discontinuous region of the Rayleigh regime as well as the surface disturbance and discontinuous regions of the first wind-induced regime. Due to its prohibitively complex nature of models proposed in the literature, this phenomenon was not treated in the present analysis.

Research implies that the inclusion of this phenomenon would increase the surface area calculated in the aforementioned regimes. As such, its omission represents a more conservative estimate of the surface area – leading to a proportionally conservative estimate of heat transfer.

Bibliography

1. ALSTOM Technology Ltd. 2006. Method and apparatus for thermal degassing. U.S. Patent 7,074,259, filed March 12, 2004, and issued July 11, 2006.

2. Benedeck, S. International Journal of Heat and Mass Transfer, Vol. 19, 1976, pp. 448.

3. Bergwerk , W. "Flow pattern in diesel nozzle spray holes." Proceeding of the Institute of Mechanical Engineering, Vol. 173, No. 25, 1959, pp. 655-660.

4. Bidone, G. *Experiences sur la Forme et sur la Direction des Veines et des Courants d'Eau Lances par Diverses Ouvertures*. Turin: Imprimerie Royale, 1829.

5. Castleman, R. "The mechanism of the atomization of liquids." Journal for the Research of the National Bureau of Standards, Vol. 6, No. 281, 1931, pp. 369-376.

6. Celata, G., Cumo, M., Farello, G., and Focardi, G. "A comprehensive analysis of direct contact condensation of saturated liquid steam on subcooled liquid jets." International Journal of Heat & Mass Transfer, Vol. 32, No. 4, 1989, pp. 639-654.

7. Chigier, N., and Reitz, R. "Regimes of jet breakup and breakup mechanisms (physical aspects)." Progress in Astronautics and Aeronautics, Vol. 166, 1996, pp. 109-135.

8. Collier, J., and Thome, J. *Convective Boiling and Condensation, 3rd Edition*. Oxford: Oxford University Press, 2001.

9. DeJuhasz, K. Transactions of the American Society of Mechanical Engineers, Vol. 53, 1931, p. 65.

10. DeSalve, M., et al. *Proceedings of the 8th International Heat Transfer Conference*. San Francisco, Vol. 4, 1986, pp. 1653.

11. Dumouchel, C. "On the experimental investigation on primary atomization of liquid streams." Experimental Fluids, Vol. 45, 2008, pp. 371-422.

12. Eisenklam, P., and Hooper, P. "The flow characteristics of laminar and turbulent jets of liquid." Ministry of Supply D.G.G.W., Report EMR 58/10, 1958.

13. Grant, R., and Middleman, S. "Newtonian jet stability." American Institute of Chemical Engineering Journal, Vol. 12, No. 4, 1966, pp. 669-678.

14. Haenlein, A. "Ueber den zerfall eins fluessigkeitstrahles." (The disintegration of a liquid jet). National Advisory Committee on Aeronautics, 1931, Technical Notation 659.

15. Harmon, D. "Drop Sizes from Low Speed Jets." Journal of the Franklin Institute, Vol. 259, No. 5, 1955, pp. 519-522.

16. Hinze, J. *Turbulence, 2nd Edition*. New York: McGraw-Hill, 1975.

17. Hoyt, J., and Taylor, J. "Wavers on water jets." Journal of Fluid Mechanics, Vol. 83, 1977, pp. 119-127.

18. Iciek, J., Cywinska, U., and Blaszczyk, R. "Hydrodynamics of free-liquid jets and their influence on heat transfer." In *Handbook of Heat and Mass Transfer*, *Vol. 1*. Houston: Gulf, 1986, pp. 151-181.

19. Incropera, F., and Dewitt, D. *Fundamentals of Heat and Mass Transfer, 5th Edition*. Hoboken: John Wiley & Sons, Inc., 2002.

20. Isachenko, V., and Solodov, A. Teploenergetika, Vol. 18, No. 2, 1971, pp. 7.

21. Kerst, A., Judat, B., Schlunder, E. "Flow regimes of free jets and falling films at high ambient pressure." Chemical Engineering Science, Vol. 55, 2000, pp. 4189-4208.

22. Kim, S., and Mills, A. *Transactions of the ASME, Journal of Heat Transfer*, Vol. 111, 1989, pp. 1068.

23. Kutateladze, S. *AEC-TR-3770, 2nd Edition*. 1952. English translation by: US AEC.

24. Lefebvre, A. *Atomization and Sprays*. New York: Hemisphere, 1989.

25. Lin, S., and Reitz, R. "Drop and spray formation from a liquid jet." Annual Review of Fluid Mechanics, Vol. 30, 1998, pp. 85-100.

26. Liu, H. *Science and Engineering of Droplets: Fundamentals and Applications*. New York: Noyes, 1999.

27. Mahoney, T., and Sterling, M. "The breakup length of laminar newtonian liquid jets in air." Proceedings of the First International Conference on Liquid Atomization and Spray Systems, Tokyo, 1978, pp. 9-12.

28. McCarthy, M., and Molloy, N. "Review of stability of liquid jets and the influence of nozzle design." The Chemical Engineering Journal, Vol. 7, 1974, pp. 1-20.

29. Miesse, C. "Correlation of experimental data on the disintegration of liquid jets." Industrial and Engineering Chemistry, Vol. 47, No. 9, 1955, pp. 1690-1701.

30. Ohnesorge, W. "Formation of drops by nozzles and the breakup of liquid jets." Zeitschrift Angewesen Mathematica und Mechanic, Vol. 16, 1936, pp. 355-358.

31. Phinney, R. "The Breakup of a Turbulent Liquid Jet in a Gaseous Atmosphere." Journal of Fluid Mechanics, Vol. 60, 1973, pp.

32. Plateau, J. "Statique Experimentale et Theorique des Liquides Soumis aux Seules Forces Moleculaires." Cited by Rayleigh, Lord in *Theory of Sound, Vol. 2*. New York: Dover, 1945.

33. Rayleigh, Lord. "On the capillary phenomena of jets." Proceedings of the Royal Society of London, Vol. 29, 1879, pp. 71-97.

34. Reitz, A., and Bracco, F. "Mechanism of atomization of a liquid jet." Physics of Fluids, Vol. 25, No. 2, 1982, pp. 1730-1741.

35. Reitz, R. *Atomization and Other Breakup Regimes of a Liquid Jet*, Ph. D. Thesis, Princeton University, 1978.

36. Reitz, R., and Bracco, F. "Mechanisms of breakup of round liquid jets." In *The Encyclopedia of Fluid Mechanics.* Houston: Gulf, 1986, pp. 233-249.

37. Sadek, R. "Communication on flow pattern in nozzle spray holes and discharge coefficient of orifices." Proceedings of the Institute of Mechanical Engineering, Vol. 173, No. 25, 1959, pp. 671-672.

38. Sallam, K., and Faeth, G. "Surface properties during primary breakup of turbulent liquid jets in still air." American Institute of Aeronautics and Astronautics Journal, Vol. 41, No. 8, 2003, pp. 1514-1524.

39. Sallam, K., Dai, Z., and Faeth, G. "Liquid breakup at the surface of turbulent round liquid jets in still gases." International Journal of Multiphase Flow, Vol. 28, 2002, pp. 427-449.

40. Sauter, J. "Determining size of drops in fuel mixture of internal combustion engines." National Advisory Committee on Aeronautics, 1926, Technical Memorandum 390.

41. Savart, F. Ann. Chim. Phys., Vol. 53, 1833, pp. 337-386.

42. Schiller, L. "Untersuchungen ueber Laminare und Turbulente Stromung." VDI Forschungsarbeit, Vol. 248, 1922.

43. Schweitzer, P. "Mechanism of disintegration of liquid jets." Journal of Applied Physics, Vol. 8, 1937, pp. 513-521.

44. Shah, R., and Sekulic, D. "Heat exchangers." In *Handbook of Heat Transfer, 3rd Edition.* Boston: McGraw-Hill, 1998, pp. 17.1-17.169.

45. Shibata, K., Koshizuka, S, and Oka, Y. "Numerical analysis of jet breakup behavior using particle method." Journal of Nuclear Science and Technology, Vol. 41, No. 7, 2004, pp. 715-722.

46. Shimizu, M., Arai, M., and Hiroyuki, H. "Measurements of breakup length in high speed jet." Bulletin of JSME, Vol. 27, No. 230, 1984, pp. 1709-1715.

47. Sklover, G., and Rodivilin, M. Thermal Engineering, Vol. 23, No. 4, 1976, pp. 30.

48. Smith, S., and Moss, H. Proceedings of the Royal Society of London, Vol. 93, 1917, pp. 373.

49. Sterling, A., and Sleicher, C. "The instability of capillary jets." Journal of Fluid Mechanics, Vol. 68, 1975, pp. 477-495.

50. Takahashi, M., Fujinuma, H., Tsukui, J., and Inoue, A. "Experimental study on condensation heat transfer on surface of liquid jet." Journal of Nuclear Science and Technology, Vol. 29, No. 8, 1992, pp. 721-734.

51. Tanasawa, Y., and Toyoda, S. "On the Atomization of Liquid Jet Issuing from a Cylindrical Nozzle." The Technology Reports of the Tohoku University, No. 19-2, 1954, pp. 135-156.

52. Teng, H., Kinoshita, C., and Masutani, S. "Prediction of droplet size from the breakup of cylindrical liquid jets." International Journal of Multiphase Flow, Vol. 21, No. 1, 1995, pp. 129-136.

53. Tomotika, S. "On the instability of a cylindrical thread of a viscous liquid surrounded by another viscous fluid." Proceedings of the Royal Society of London, Vol. A150, pp. 322-337.

54. Tyler, E. "Instability of liquid jets." Philosophical Magazine, Vol. 16, 1933, pp. 504-518.

55. Van de Sande, E., and Smith, J. "Jet breakup and air entrainment by low-velocity turbulent jets." Chemical Engineering and Science, Vol. 31, No. 3, 1976, pp. 219-224.

56. Weber, C. "Disintegration of liquid jets." Zeitschrift Angewesen Mathematica und Mechanic, Vol. 2, 1931, pp. 136-141.

57. Wu, P., and Faeth, G. "Onset and end of drop formation along the surface of turbulent liquid jets in still gases." Physics of Fluids, Vol. 7, No. 11, 1995, pp. 2915-2917.

58. Wu, P., Tseng, L., and Faeth, G. "Primary breakup in gas/liquid mixing layers for turbulent liquids." Atomization and Sprays, Vol. 2, 1992, pp. 295-317.

59. Young, M., and Bajorek, S. "The effect of noncondensables on condensation in reactor LOCA transients." *AICHE Heat Transfer Conference*, Baltimore, 1997.